UNDERSTANDING THE GROWTH MECHANISM OF PbSe NANORODS

Shailendra Chiluwal

A Thesis

Submitted to the Graduate College of Bowling Green
State University in partial fulfillment of
the requirements for the degree of

MASTER OF SCIENCE

August 2016

Committee:

Liangfeng Sun, Advisor

Lewis P. Fulcher

Mikhail Zamkov

ABSTRACT

Liangfeng Sun, Advisor

Colloidal nanomaterials have been of great interest due to their unique optoelectronic properties. The shape and size tuning of the nanomaterials at nanometer scale results in novel optical and electronic properties. Due to a high conductivity and large multiple exciton generations, PbSe nanorods are considered great for optoelectronic applications. We have developed a procedure for nanorods synthesis. TEM images, photoluminescence, absorption and PL lifetime peaks show that the rods produced are of high quality. We have studied the role of temperature and growth time on size tuning of PbSe nanorods. We have also studied the effect of the amount of chloroalkane, the ratio of oleic acid to lead, the amount of acetic acid and water on PbSe nanorods.

To My Family

ACKNOWLEDGMENTS

I would like to express my sincere gratitude to my thesis supervisor Dr. Liangfeng Sun for providing me an opportunity to work under his supervision. I would like to acknowledge all the group members for their continuous support. I am also thankful for funding by Physics and Astronomy department. Finally, I would like to thank my family for their constant inspiration throughout my study.

TABLE OF CONTENTS

LIST OF FIGURES

LIST OF TABLES

CHAPTER 1: INTRODUCTION

1.1 GENERAL INTRODUCTION OF NANOSCIENCE

From the last three decades, a branch of science known as nanoscience has been developed which has a great impact on different fields like material science, medicine, technology, and industry. Nanoscience deals with the nanomaterials, which have sizes of the nanometer scale. After the invention of the tunneling electron microscope[1] in the1980s, it was easier to see materials on the nanometer scale, which helped in the growth of nanoscience. When the materials are at nanoscale, their physical, chemical and biological properties differ from the fundamental properties of materials than when they are in bulk state. Thus, they show a lot of unique characteristics, which make them good candidates for potential applications such as solar cells, photo diodes, transistors, [1-4] and sensors[5-7]. Besides this, these nanomaterials can be used for industrial applications like self-cleaning surfaces 2. In the medical field, nanomaterials are used to diagnose diseases[8] and also to study proteins, which are responsible for carrying the genetic information[7-10]

1.2 QUANTUM CONFINEMENT

As the size of the materials changes from bulk to the nanoscale, materials will have dimensions comparable to the exciton Bohr radius, increasing the surface to volume ratio, which results in a change in electric, thermal, magnetic and optical properties[11] of the materials. When the electrons in the nanomaterials are squeezed to the size comparable to exciton Bohr radius, the overlapping energy orbitals of nanomaterials change to discrete energy levels. [12, 13] This phenomenon is known as quantum confinement. Quantum confinement is dependent on the size of the materials. As the

size of the material is reduced below the exciton Bohr radius, the quantum confinement effect is stronger and vice versa. The Bohr radius of the material depends on the dielectric screening and the periodic lattice structure of the materials. [14, 15] The formula to calculate Bohr radius [15] (a_0) is:

$$a_0 = \frac{\varepsilon \hbar^2}{2m^* e^2}$$

Where, ε = the dielectric constant of the semiconductor

m* = the effective mass of the electron or hole

$\hbar$ = reduced Planck's constant

e = charge of electron

Depending on the structural dimensions, nanomaterials can be categorized into three groups, o-dimensional quantum dots, 1-dimensional nanorods or nanowires, and 2-dimensional nanosheets. [16] The quantum dots, nanorods, and nanowires have different kinds of quantum confinement. Quantum dots have 3-dimensional quantum confinement, nanorods have 2-dimensional quantum confinement and nanosheets have 1-dimensional quantum confinement. The figure below shows the relationship between the density of the state (DOS) and the structural dimension of the nanomaterial. [16]

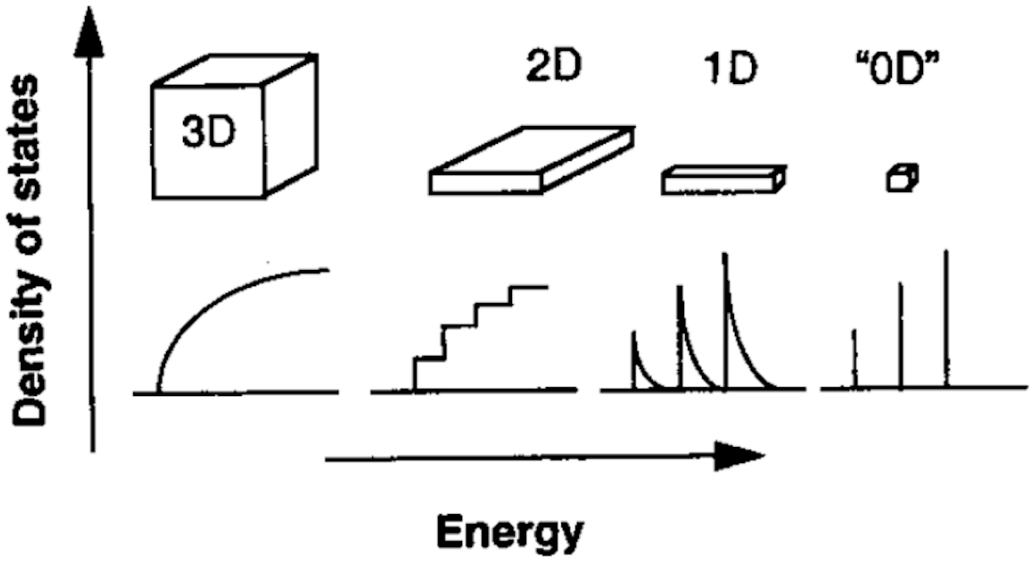

Figure 1.1: Density of the states and energy as a function of structural dimension of materials

Quantum confinement also depends on the type of the material used, since the exciton Bohr radius is different for different types of materials. Below the Bohr radius, the material will behave as a semiconductor with wide band gap. The Bohr radii for some materials is listed in Table 1.1. [17]

Material	Bohr Radius (nm)
CuCl	1
CdSe	6
PbS	20
InAs	34
PbSe	46
InSb	54
PbTe	46

Table 1-1: Bohr radii of some materials

The physics of excitons depends on size as well as the shape of the nanomaterials. It has been observed that at the same volume for PbSe nanorods; the biexciton Auger lifetime is six times longer than the lifetime for quantum dots. [18] Also, the biexciton lifetime is found to be 3 to 4 times larger than that of quantum dots.[19]

1.3 OBJECTIVE OF THIS PROJECT

Due to potential applications in optoelectronics, PbSe nanorods are of great interest for researchers in the field of the nanoscience. [20-25] PbSe nanorods are found to have reduced Auger recombination rates, [18, 26, 27] high multiple exciton generation rates[18, 28, 29], large exciton Bohr radius, [30-32] and large Dtokes' shifts. [33, 34] Nanorods of the various aspect ratios from 1.5 to 12 nm have been synthesized using different methods. [18, 19] For the nanorods to be used in optoelectronics, they should be of high quality. The synthesis method developed by Koh et al. [35] has been used in the synthesis of the PbSe nanorods nowadays by a lot of researchers in this field. The colloidal synthesis method developed has lots of organic and inorganic chemicals involved throughout the synthesis process. The different groups have reported the effect of different chemicals involved in the reaction for example Cho et al.[36] have studied the effect of temperature on growth, Boercker et al.[37] have studied the effect of water, Houtepen et al.[38] have studied the effect of acetate on PbSe nanocrystals, Dai et al.[39] have studied the effect of ligands on PbSe nanocrystals. In this project, we have studied the effect of each chemical on the formation of the PbSe nanorods, so that we can understand the growth mechanism. For this, we have developed a method of nanorod synthesis and from that synthesis method; we have changed parameters like the amount of chloroalkane, the oleic acid to lead ratio, the amount of acetic acid and water.

1.4 SYNTHESIS OF NANOMATERIALS

Nanoscience is considered more advanced technology because of cost effectiveness for the synthesis of nanomaterials. There are two well-known approaches for the synthesis of nanomaterials.

1.4.1 Top-Down Approach:

In this approach, the bulk material is taken, and by using a physical or a chemical method, its crystal planes are removed to make nanomaterials. This method is not considered very good because of more defects, and less control over size as well as shape. [40, 41]

1.4.2 Bottom-Up Approach:

In this approach, attaching atoms, molecules or crystal planes in specific directions forms nanomaterials. This method is considered often better than Top-down because of high reproducibility, fewer defects, and better control over size as well as shape.[42-44]

In our project, we have used Bottom-up approach. For this, we have used the colloidal synthesis method. In this method, two precursor solutions are prepared and mixed at the desired conditions. This method is easy to use as we have control over almost all of the parameters, like pressure, temperature, and time, involved in the synthesis method.

CHAPTER 2: EXPERIMENTAL METHODS

In this chapter, the experimental details for the synthesis of PbSe nanorods, characterization methods we have used in our project are discussed.

2.1 SYNTHESIS OF PbSe NANORODS (NRs)

For the synthesis of nanorods, we have followed two methods and have adjusted some reaction conditions. One is developed by Bhandari et. al.[44] and other is by Zhang et al. [45] The main difference in these methods is the lead precursor.

2.1.1 With acetate:

For the synthesis of nanorods with acetate, we followed the procedure reported by Bhandari et. al. [44] with a slight modification of the precursor. We used selenium powder instead of thioacetamide. In a typical single pot synthesis, both the precursor solutions are made and mixed together. For this synthesis, lead (Pb) precursor was prepared by using 860 mg (2.27 mmol, 99.999%) lead (II) acetate trihydrate, 3.5 ml (12.4 mmol, 90%) oleic acid (OA) and 10 ml diphenyl ether (DPE-99%). All of these chemicals were added to one three-necked flask and heated to 85^0C under continuous nitrogen flow. Once the temperature reached 85^0C, the vacuum was started and was degassed for 2 hours. Degassing is done to remove water and acetic acid present in the lead oleate solution. After degassing, the temperature was increased to the desired temperature. Here the desired temperature was determined by the boiling point of chloroalkane. It is usually 5^0C below the boiling point of chloroalkane. At that temperature, the chloroalkane was added. The reaction was carried out for half an hour. Then the temperature was increased to 20^0C more than the boiling point of the chloroalkane and the selenium precursor was added.

At the same time, the selenium (Se) precursor was prepared in another three-necked flask at room temperature. For this, 12.6 mg (0.016 mmol, 99.99%) of selenium powder and 70 μl of N, N-dimethylformamide (DMF, 99.8%) were collected in one flask and kept under nitrogen flow for some time. Then 930 μl of trioctylphosphine (TOP, 90%) was added to solution and then it was mixed for 25-30 minutes to form TOPSe. All the chemicals were purchased from Sigma-Aldrich except DMF, which was purchased from EMD chemicals.

Once the Pb and Se were added together, the mixture was mixed vigorously. The color of the sample started to change from pale yellow to dark brown indicating the formation of nanocrystals. Samples were taken at different growth times ranging from 30 second to 5.5 min and the samples formed were quenched in 15 ml of toluene to stop the growth. The samples collected were precipitated using 10 ml of methanol under centrifuge (3.5 krpm) for 5 min. The precipitated sample was dried and re-dispersed in toluene, and this precipitation method was repeated for three times.

In the table below, the list of chloroalkanes we used, their boiling points and final mixing temperatures are shown.

Chloroalkane	Boiling Point	Mixing Temperature
1,2-Dichloropropane (DCP)	95-96^{0}C	110^{0}C
1,1,2-Trichloroethane (TCA)	114^{0}C	130^{0}C
1,2-Dichlorobutane (DCB)	134^{0}C	150^{0}C
1,2,3-Trichloropropane (TCP)	156^{0}C	170^{0}C

Table 2-1: List of chloroalkanes used, boiling point of each chloroalkane and corresponding mixing temperature.

2.1.2 Without Acetate:

The success rate for above mentioned synthesis was not good. A possible reason for the low success rate could be due to the presence of acetic acid while the lead oleate was formed. So a new synthesis method was developed, which was acetate free. For this, we used the method developed by Zhang et al. [45], with a slight modification after degassing. For this, the lead precursor was prepared using lead (II) oxide instead of lead (II) acetate trihydrate. 506 mg (2.27 mmol) lead (II) oxide, 1.8 ml (6.38 mmol) oleic acid and 10 ml of DPE were mixed and heated to 110^0C under the nitrogen environment until the solution turned clear. Then the temperature was reduced to 100^0C, and degassing was done for 20 minutes. In this case degassing was done to remove water. After degassing we followed the same procedure as mentioned above, and the Se precursor was also prepared in a similar way. Samples were prepared, precipitated and collected as discussed in 2.1.1.

2.2 PHOTOLUMINESCENCE SPECTROSCOPY

A technique to measure light emitted from any material after the absorption of photons is known as photoluminescence (PL) spectroscopy. When sample absorbs the photon, both PL and Raman scattering can occur. PL is stronger than Raman scattering. PL is the combination of both fluorescence and phosphorescence processes. It originates due to absorption or emission processes between different energy levels in the material. The figure below gives the schematic representation of PL.[46]

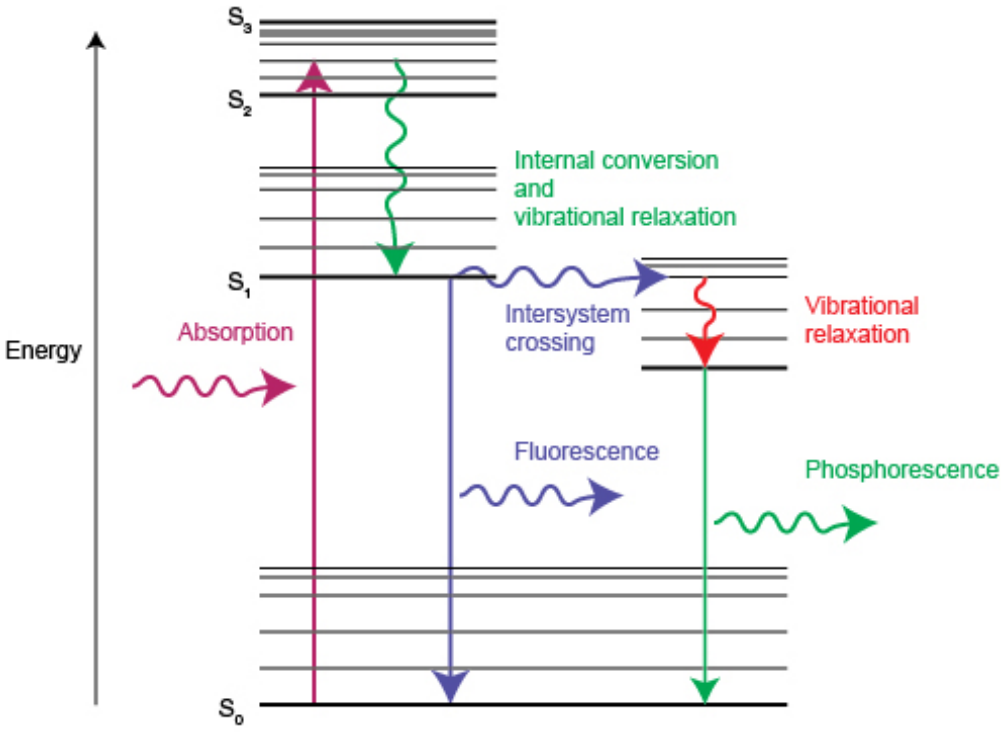

Figure 2.1: Schematic representation of fluorescence and phosphorescence

To study the PL of the nanorods a home built PL Spectroscopy apparatus is used, consisting of an argon laser, a monochromator, and an IR detector. Two mirrors and two irises were used to align the laser beam to shoot at the specimen. The continuous laser signal was pulsed using a chopper, and the laser intensity was controlled using the filter. Two convex mirrors were used to converge the emitted light from the specimen. A band-pass filter was also used before the detector to cut off the certain wavelength. From the detector, signals were sent to a lock-in amplifier and then to a computer to convert the signals into digital data. The software, programmed in LabVIEW, was used to control the measurements. The schematic diagram of PL system is shown in Figure 2.2. [47-50]

Nanorods were dispersed in tetrachloroethene (TCE) and were kept in a quartz cuvette for the measurements.

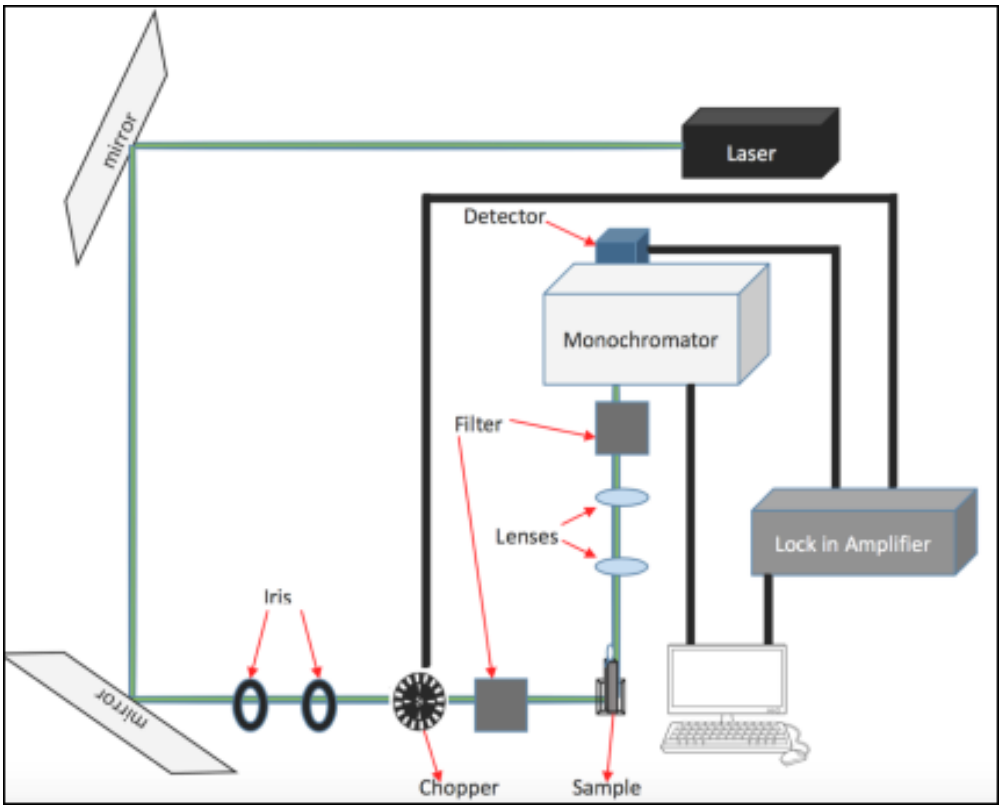

Figure 2.2: Schematic diagram for home-built photoluminescence spectroscopy

2.3 ABSORPTION MEASUREMENTS

When light is passed through a material, it absorbs the light and the amount of absorption depends on materials and conditions under which the materials are synthesized. To measure the absorption of the nanorods a homemade system was used. This measurement is important; it is directly related to the band gap energy of the nanorods. For the absorption measurement nanorods, the sample was dispersed in TCE and kept in a cuvette. Also, another cuvette with TCE only was used as a reference. According to Beer-lambert law, the absorption of the light can be calculated as: [51]

$$A = \log\left(\frac{I_0}{I}\right)$$

Where,

A = Absorption of light at a particular wavelength

I_0 = the intensity of the light without any sample

I = intensity of light after passing through the sample

2.4 PHOTOLUMINESCENCE LIFETIME MEASUREMENT

When a specimen absorbs the photons, the electrons in the specimen go to the excited state. The excited electrons again go back to the ground state by emitting other photons. The average time for the electrons to go back to ground state after the absorption of the photons is known as the photoluminescence lifetime. The technique to study this decay time is known as photoluminescence lifetime spectroscopy. For nanorods a single exponential decay has been observed. This lifetime can be calculated from the equation[52]

$$I(t) = I_0 e^{(-t/\tau)}$$

Where, I_0 = intensity of electron at time t = 0

I (t) = intensity of electron at time t

τ = decay time

Based on the above equation, the lifetime is defined as the time taken by an excited population to decay to 1/e or 37% of the initial intensity.

The benefit of using PL lifetime measurement is that the concentration of the sample doesn't affect the lifetime. For the PL lifetime measurement, a short pulse of the light source is used to excite the sample. The intensities of fluorophores at time t = 0 and at time t were recorded. The recorded data

was plotted on logarithmic scale, and a single exponential fitting was used to calculate the lifetime using SciDavis software.

2.5 TRANSMISSION ELECTRON MICROSCOPY (TEM)

To confirm the morphology of the sample we synthesized, a powerful technique known as transmission electron microscopy (TEM) was used. In this technique, a beam of electrons is passed through a sample and this beam of electrons will interact with the sample, which is used to get an image of the sample. To obtain a TEM image, specially functionalized copper grids were used. A small amount of nanorod samples were dispersed in toluene and was transferred onto TEM grids. The TEM grid was allowed to dry for several minutes. A typical TEM image of nanorods is shown in Figure 2.3.

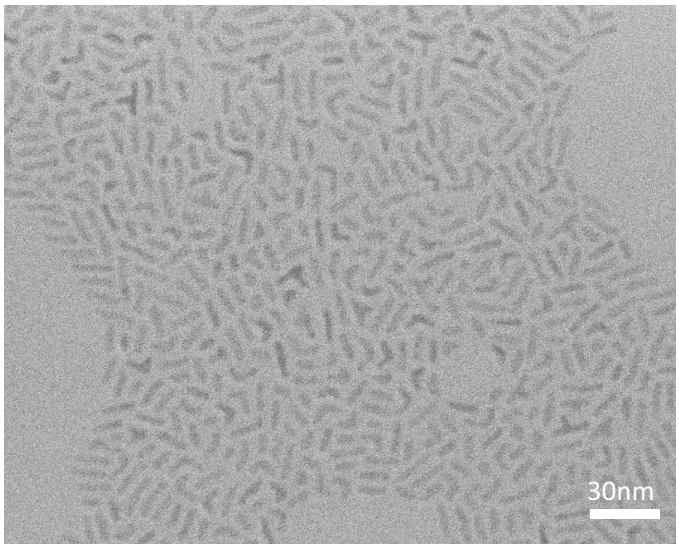

Figure 2.3: TEM image of PbSe nanorods

2.6 DIAMETER AND LENGTH MEASUREMENT OF NANOCRYSTALS

It is essential to do precise measurement of the diameter and length of the nanorods so that the growth mechanism can be well understood. The software ImageJ was used to do the statistical calculation of the diameter and length of nanorod samples. For this purpose, a high-resolution

TEM image was selected and the scale of measurement was set. The scale of the measurement depends on the scale of the TEM image; the scale on the TEM image is set by drawing a straight line on TEM image. Once the scale is set, a line is drawn across diameter or length and then ‘M’ is pressed to collect the data. More than hundred data were collected. These collected data were used for further calculation to determine the mean value and the standard deviation of the diameters and lengths. This method to measure diameter or length has its limitations, but due to the large number of data collected, the measurements follow a Gaussian distribution. Therefore, the results for the diameter and length obtained are acceptable.

CHAPTER 3: RESULTS

In this chapter, characterization of PbSe NRs and the results of the effects of different parameters including temperature, time, chloroalkane, oleic acid, acetic acid, and water are discussed

3.1 HIGH QUALITY PbSe NANORODS

The PbSe nanorods produced are uniform in diameter and have a narrow PL emission peak with full width half maxima (FWHM) of 200 nm. From the PL lifetime measurement, it is found that the lifetime of the nanorods is 823 ns. The PL lifetime graph is nearly a single exponential, which means the nanorods are of high quality.

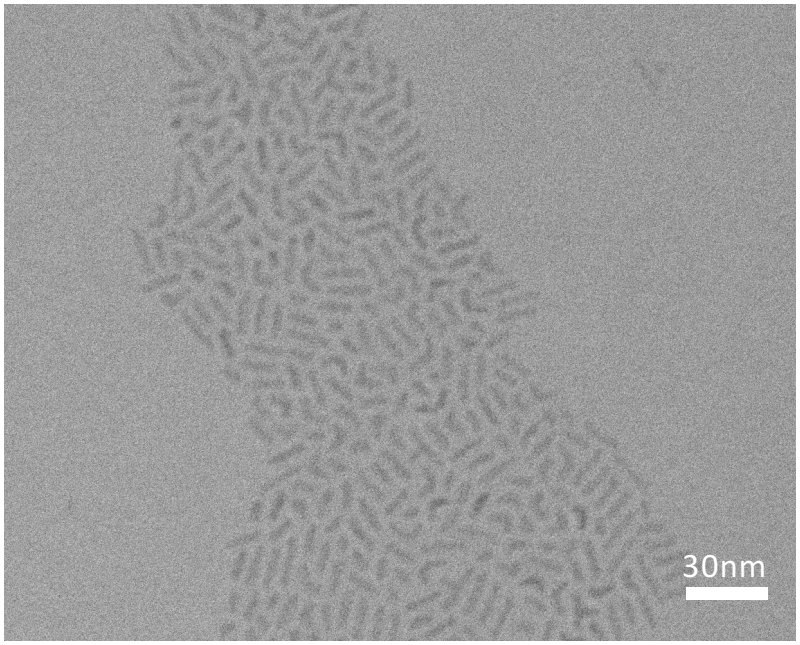

Figure 3.1: TEM image of PbSe NRs synthesized at 130^0C using TCA at 5 min.

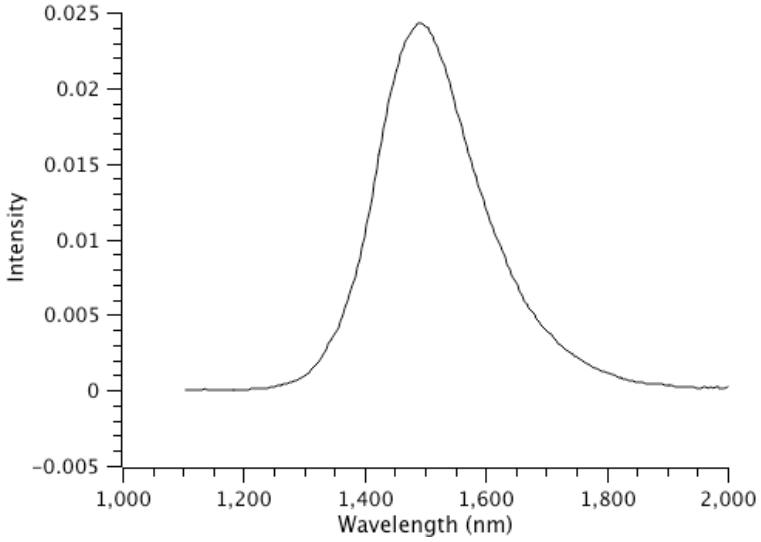

Figure 3.2: PL intensity curve of NRs shown in Figure 3.1.

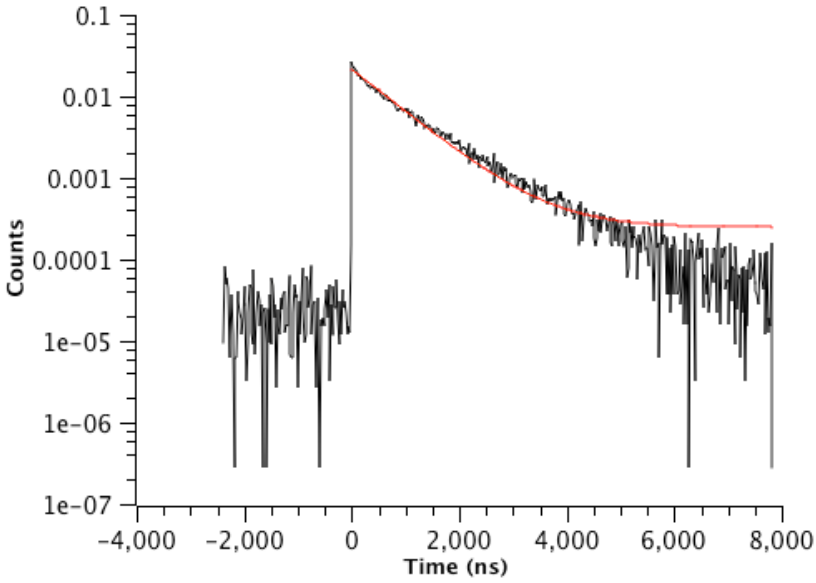

Figure 3.3: PL lifetime of NRs at peak position shown in Figure 3.1.

3.2 TIME DEPENDENT GROWTH

For this, the reaction temperature was fixed at 170^0C and TCP was used as the chloroalkane. Growth times of 40 sec to 3min were observed. Though the diameter has been increased, the aspect

ratio of the nanorods was same, indicating anisotropic growth of nanorods. From the PL data, it was observed that the PL was red-shifted, indicating the increase in diameter of the nanorods. Also, absorption shows a similar trend. [48]

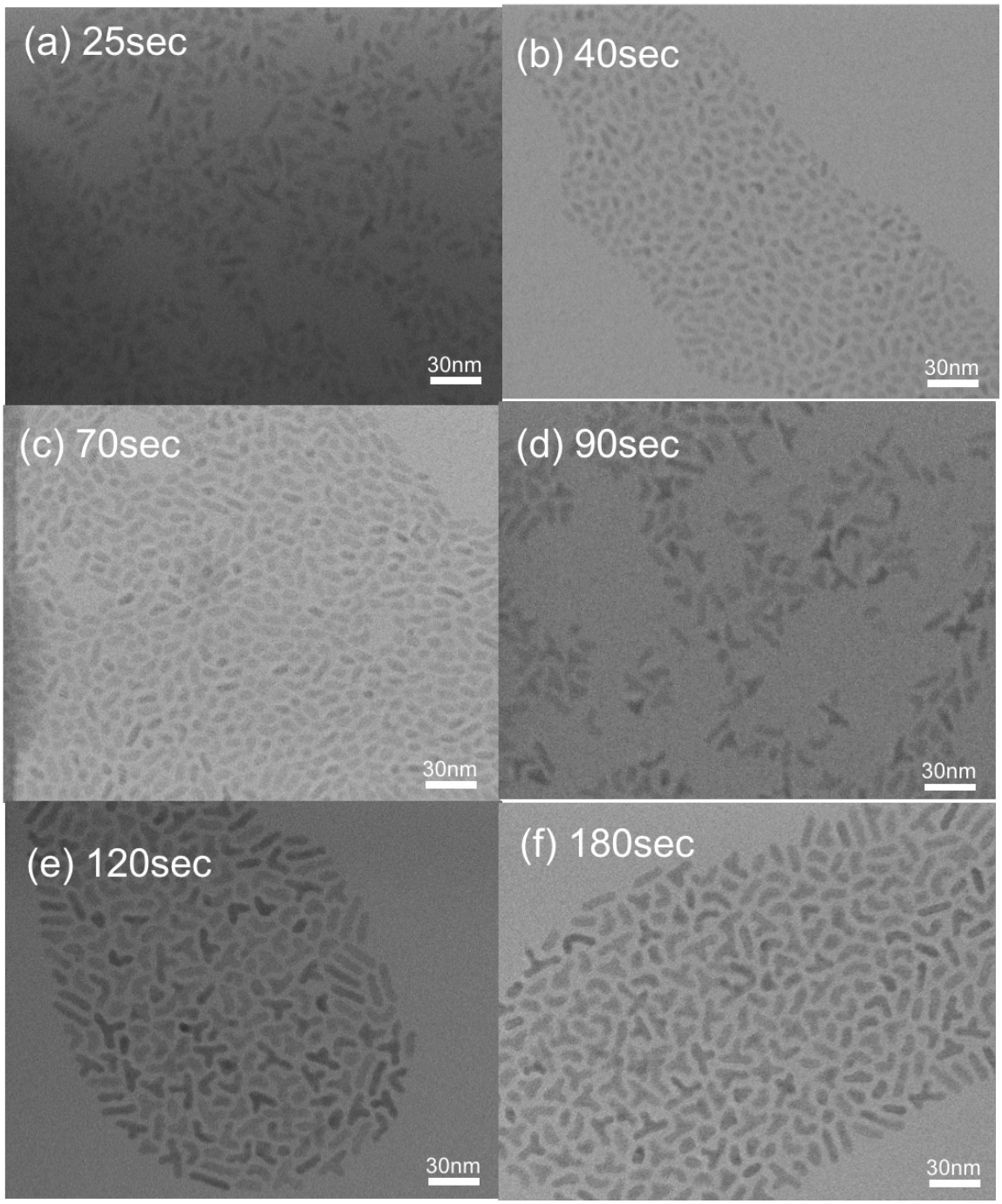

Figure 3.4: TEM images of the PbSe nanorods synthesized at 170^0C with different time as indicated in the images.

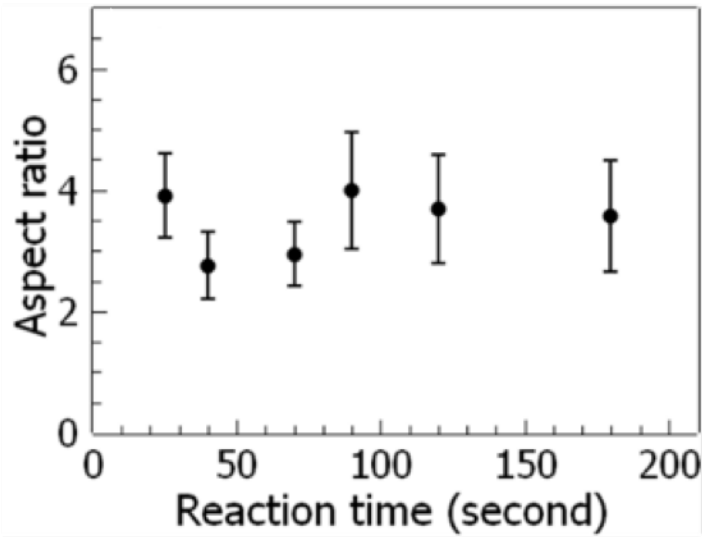

Figure 3.5: Aspect ratio of the nanorods over the reaction time.

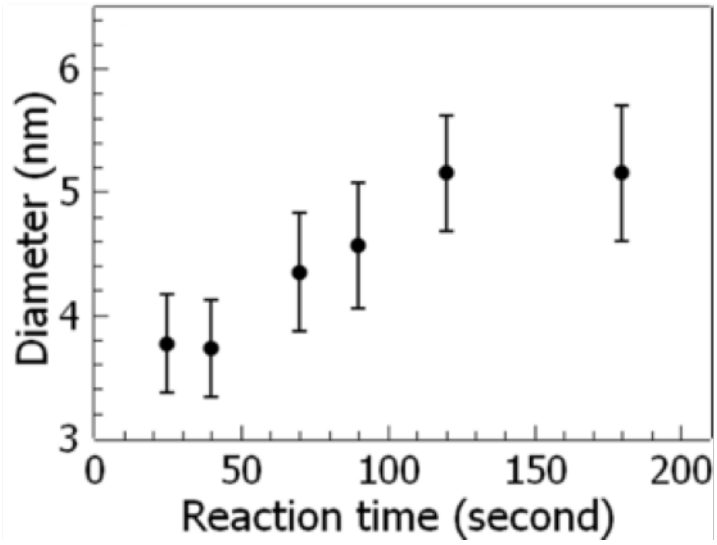

Figure 3.6: Diameter of the nanorods over the reaction time.

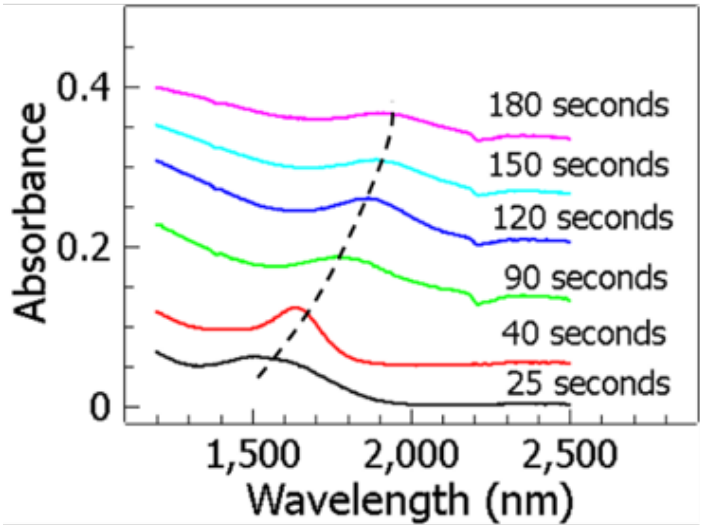

Figure 3.7: Absorbance spectra of the PbSe nanorods at different growth stages. The spectra are vertically shifted for clarity. The dashed line indicates the shift of the lowest-energy absorption peak over the reaction time.

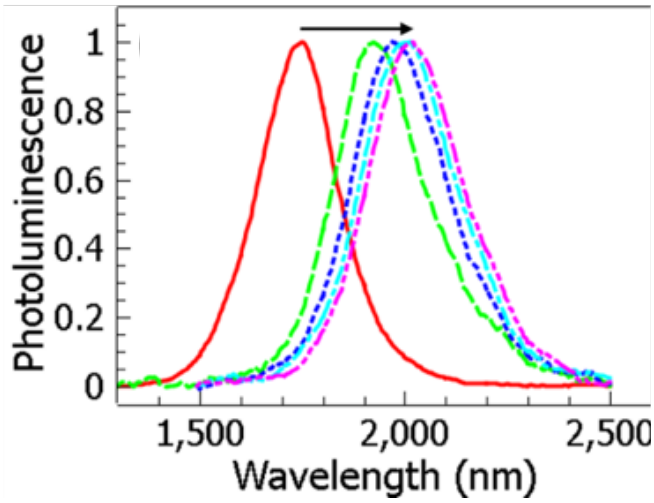

Figure 3.8: Photoluminescence spectra of the PbSe nanorods at reaction time of 40, 90, 120, 150 and 180 seconds (from left to right). The arrow indicates the red-shift of the photoluminescence peak over the reaction time.

3.3 GROWTH MECHANISM

To understand the crystal structure as well as the anisotropic growth of the nanorods high resolution TEM (HRTEM) were taken as shown in Figure 3.9.

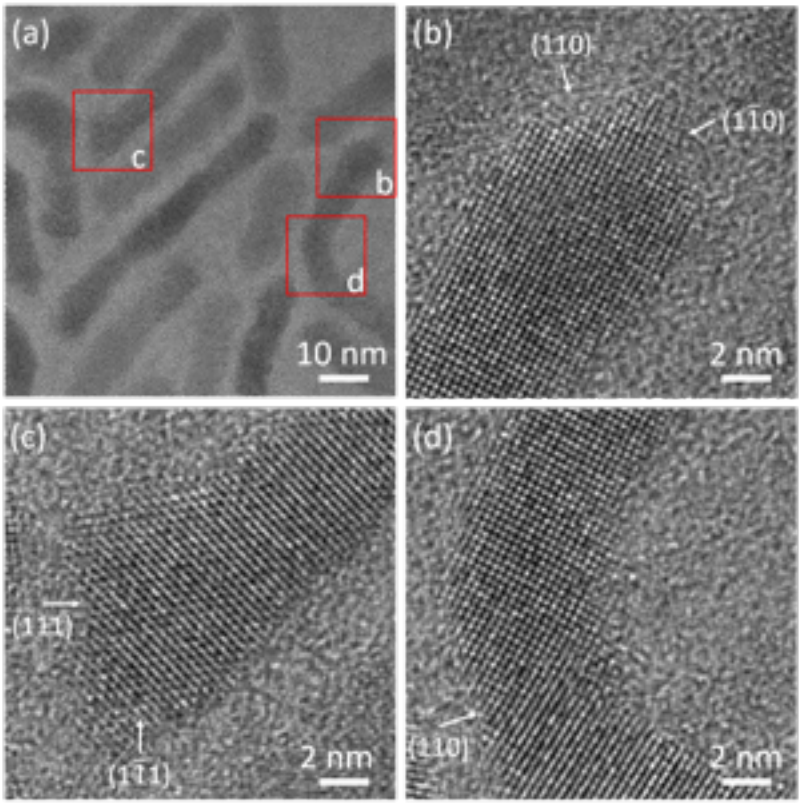

Figure 3.9: (a) TEM image of PbSe nanorods synthesized at 180 ^{o}C with TCP. The squares labeled with "b", "c" and "d" indicate the areas to be zoomed-in in (b), (c) and (d), respectively. (b) Close-up HRTEM image of the nanorod showing a rock-salt crystal structure with {100} facet facing up. The tip of the rod is formed by the (110) and the (1$\bar{1}$0) facets. (c) Close-up HRTEM image of the nanorod with its {110} facet facing up. The tip of the rod is formed by the (111) and the (1$\bar{1}$1) facets. (d) The HRTEM image of an L-shaped nanorod with its {100} facet facing up. The growth direction of the nanorod makes two 45^{o} turns and forms an L shape.

HRTEM shows that the side facets of the nanorods are either the {100} direction or the {110} direction as shown in the figures 3.9 (a) and 3.9 (c) respectively. this shows that axis of growth is in <100> or <110> direction. The projected minimum atom spacing in the axial direction for both b and c is found to be 0.31nm and in the lateral direction, it is 0.31 nm for b and 0.22 nm for c. Nanorods with axis in <110> direction also show <100> or <110> side facets, but the projected minimum atom spacing in axial or lateral direction is different. As shown in figure below:

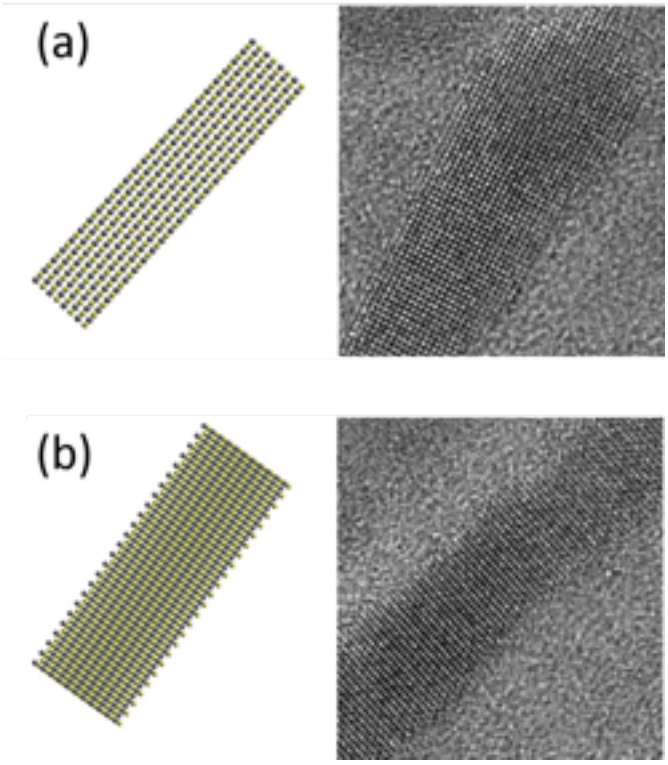

Figure 3.10: Projections of the nanorods in different zone axis.

As shown in the figure 3.9 (b) and (c), the two ends of the nanorods are not flat but they have rounded tips. The angle is about 90.0^0 in the zone axis <001> (Figure 3.9 (b)) but in the zone axis <110> (Figure 3.9 (c)) the angle is found to be 70.6^0.

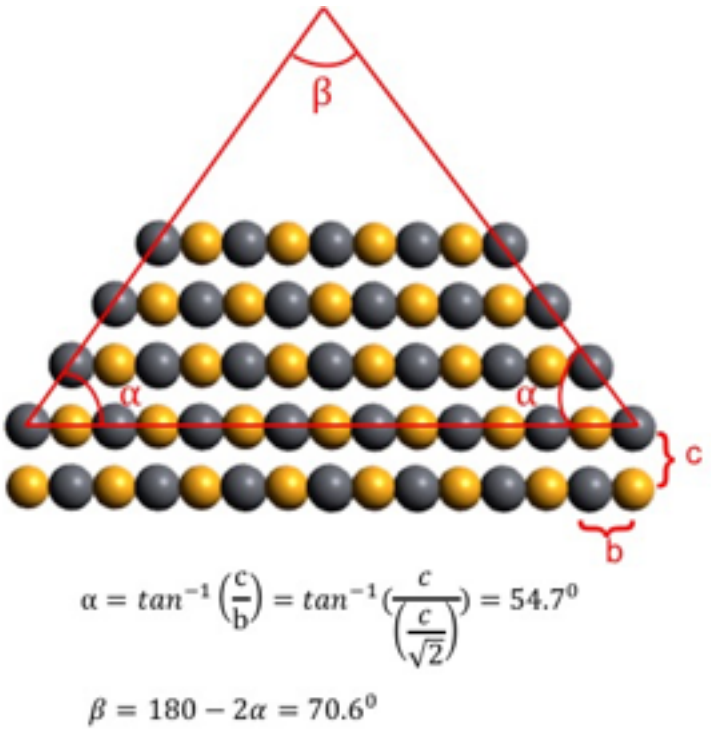

Figure 3.11: Calculation of the angle made by two {111} facets.

From HRTEM image, it's clear that ends of nanorods are mainly dominated by {110} and {111} facets. Due to more dangling bonds, the {110} and {111} facets are likely more reactive than {100} facets. We claim that a net growth in the <100> direction is due to the growth in the <110> and <111> directions. As shown in Figure 3.9 (b), the direction of growth of the {110} and $\{1\bar{1}0\}$ facets are in <110> and $<1\bar{1}0>$ respectively, which are perpendicular to each other. The crystal growth in the radial direction is reduced due to the competition among the components in <010> and $<0\bar{1}0>$ (which are opposite to each other and are perpendicular to rod axis). Although the crystal growth in radial direction is reduced, the components in <100> direction add up which enhance the net growth in <100> direction. The growth of {111} and $\{1\bar{1}\bar{1}\}$ facets (Figure 3.9 (c)) follows a similar mechanism and resulting in a net growth in <100> direction. As shown in Figure 3.9 (c), facet {111} is much larger than facet $<1\bar{1}\bar{1}>$, it's due to different growth rate in <111> and

<$1\bar{1}\bar{1}$> facets. When the difference in growth rate is large enough, the direction of growth will be changed. For L-shaped rod (Figure 3.9 (c)), the initial growth direction is <100> which turn to <110> and then to <010>.

Chloroalkanes used as cosolvents during the reaction is responsible for the one-dimensional growth. In the absence of the chloroalkanes, the nanocrystals formed are non-emissive hexapods or octahedrons.

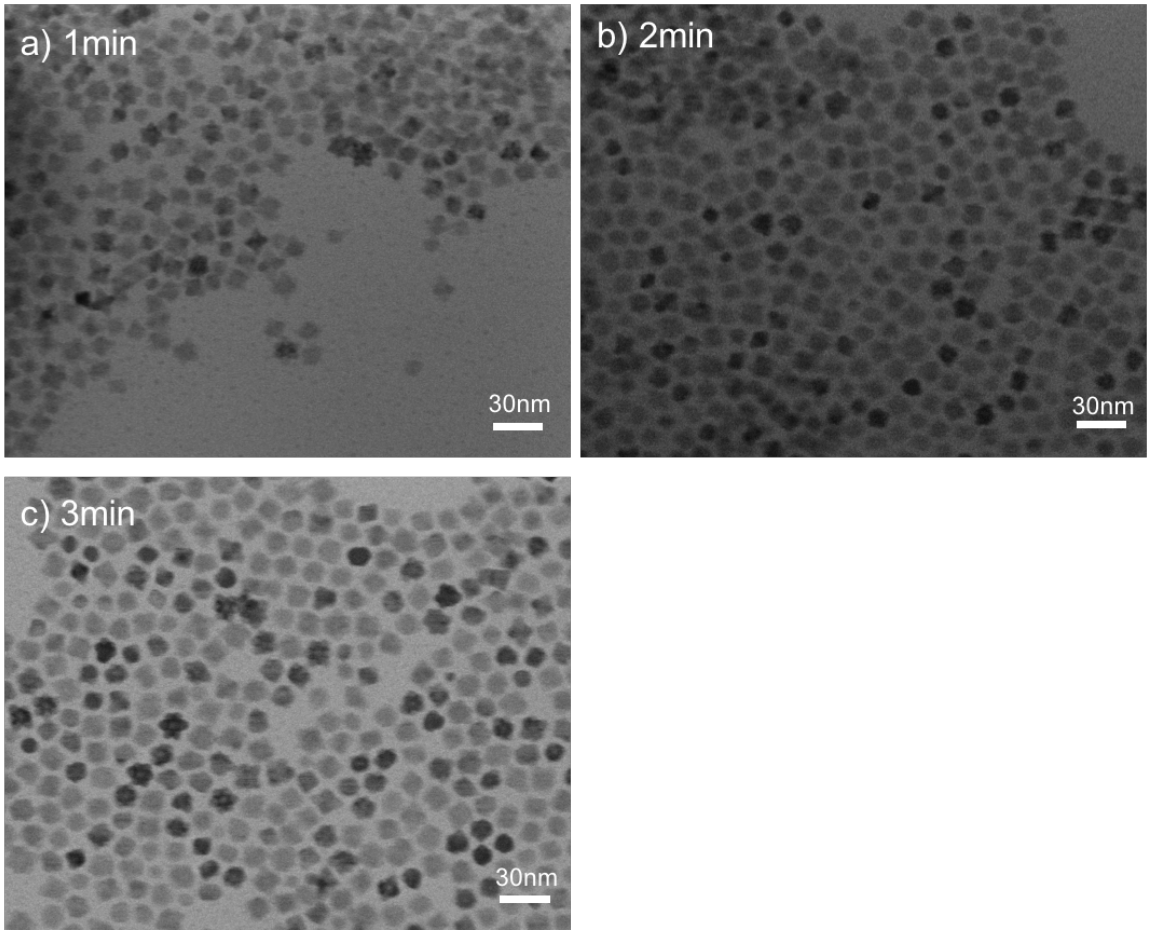

Figure 3.12: Growth of nanocrytal without chloroalkane.

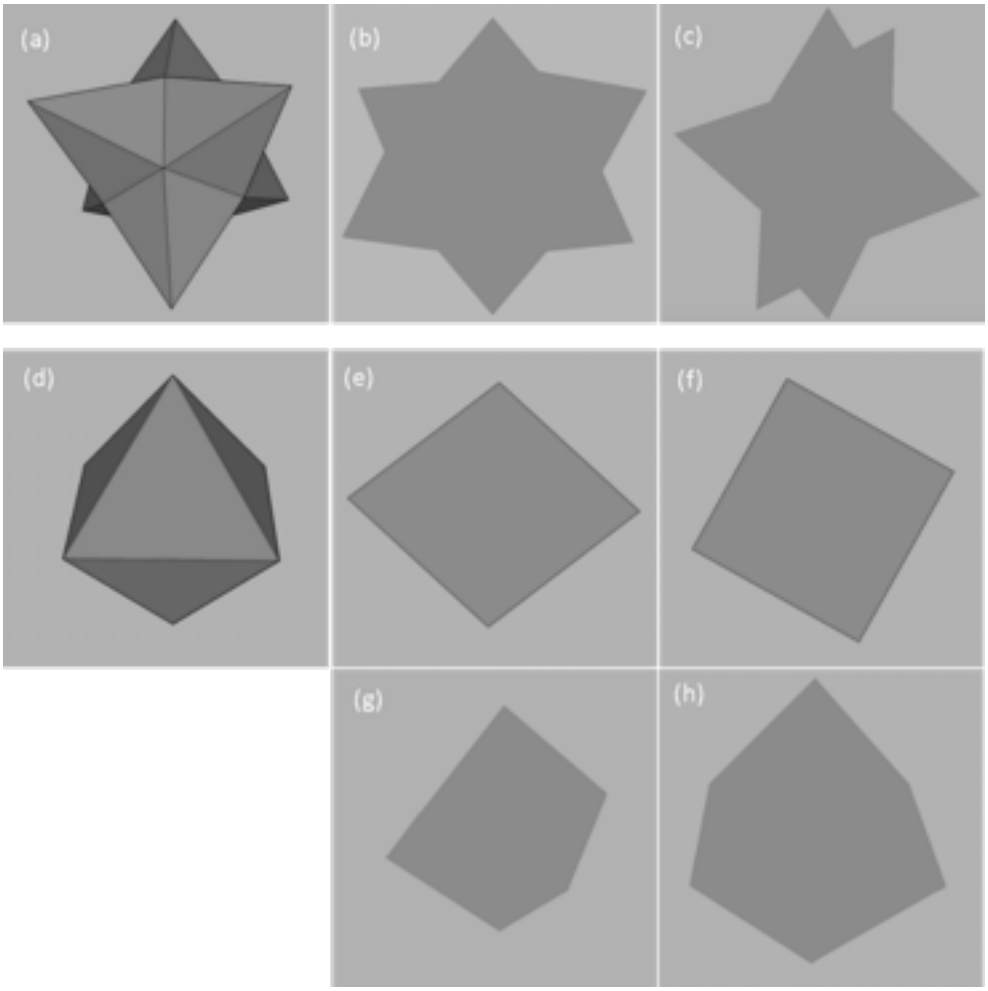

Figure 3.13: a) 3D hexapod structure and its (b, c) 2-dimensional projections. (d) 3D octahedron structure and its typical (e-h) 2-dimensional projections.

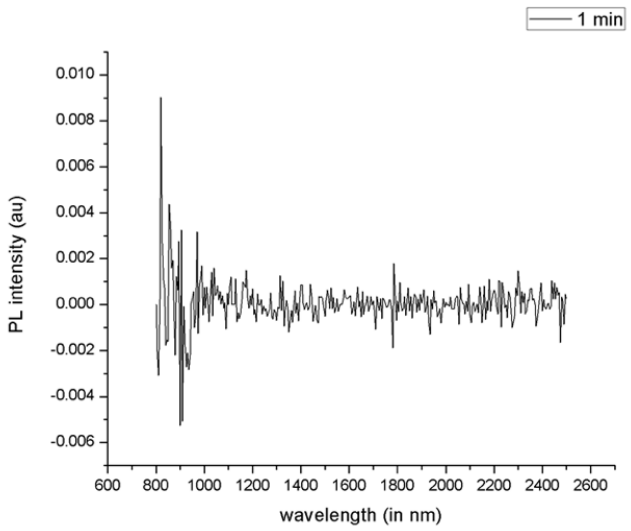

Figure 3.14: PL spectra of the nanocrystal synthesized without chloroalkane

Houtepen, [38] Gerdes, [53] and coworkers have also reported the similar structures. Gerdes and coworkers have reported that each pod of the hexapod grows in <100> direction. [53] As observed in experiments, when the chloroalkane is used it takes the longer time to observe the color change indicating the slow nucleation and growth of nanocrystal.[53, 54]The possible cause of this slowness is because chloroalkanes are lead complexing agents. [53, 54] Due to slow growth, it helped {110} and {111} facets to have higher reactivity, resulting in net growth along <100> direction.

In a cubic structure there are six equivalent <100> directions, so theoretically crystal can grow into star-shaped with six long arms. The normal I-Shaped rods indicated that they are not equivalent instead some facets are more reactive than others which are dominant for growth direction. If the reactivity of each facet is close enough to each other, growth in other directions is also possible giving L-shaped, T-shaped, Cross-shaped and even six arms shaped structure. These structures are useful to know the growth direction as some arms can point upward from the TEM grid, which makes it easier to observe crystal structure of the {100} facet, whose surface normal points to the

growth direction of the rod Figure 3.15 (a). HRTEM image (Figure 3.15) confirms that the end facet is {100} and other arms also spread in <100> direction. The HRTEM also shows that the cross-section of the rod is octagonal. The octagonal rod probably grows from a cuboctahedron (or truncated octahedron) seed[55] – a usual shape of a PbSe[56] or PbS[57, 58] nanocrystal.

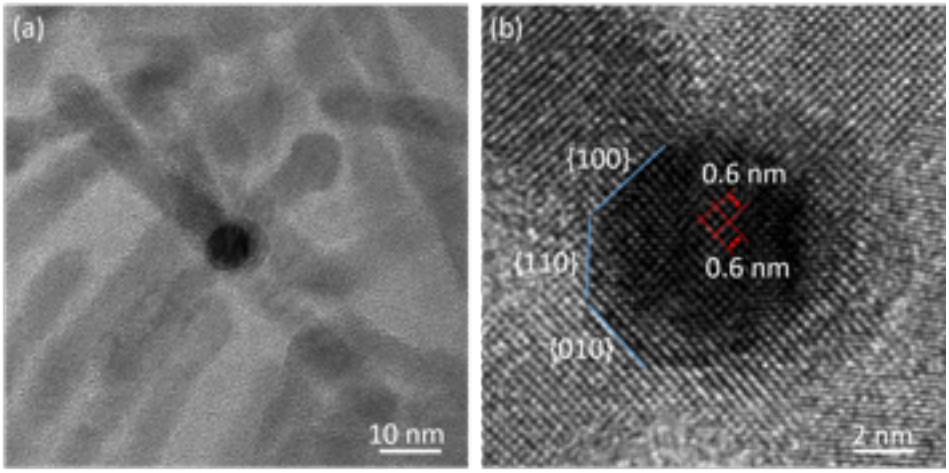

Figure 3.15: (a) A HRTEM image showing a nanorod pointing upward as the others lying down on the substrate. (b) HRTEM image of the tip of a PbSe nanorod showing a {001} facet.

3.4 TEMPERATURE DEPENDENT GROWTH

To understand how the diameter of the nanorods changes with temperature, we fixed the growth time at 3 min. Three-temperature range was taken into consideration 110^0C, 130^0C, 150^0C, 170^0C and 180^0C. We found that as the time increases the diameter of the nanorods also increases. The diameter has been tuned from 2.4 nm to 8.5 nm as the temperature increases. The reaction rate at higher temperature is really fast compared to lower temperature. At 110^0C, quantum dots, as well as nanorods, were observed and below 110^0C, no nanorods were observed indicating that this is the threshold temperature for the formation of nanorods. The reaction temperature also plays an important role in the branching of the nanorods, as seen from the TEM images there are more branches in 150^0C.[48]

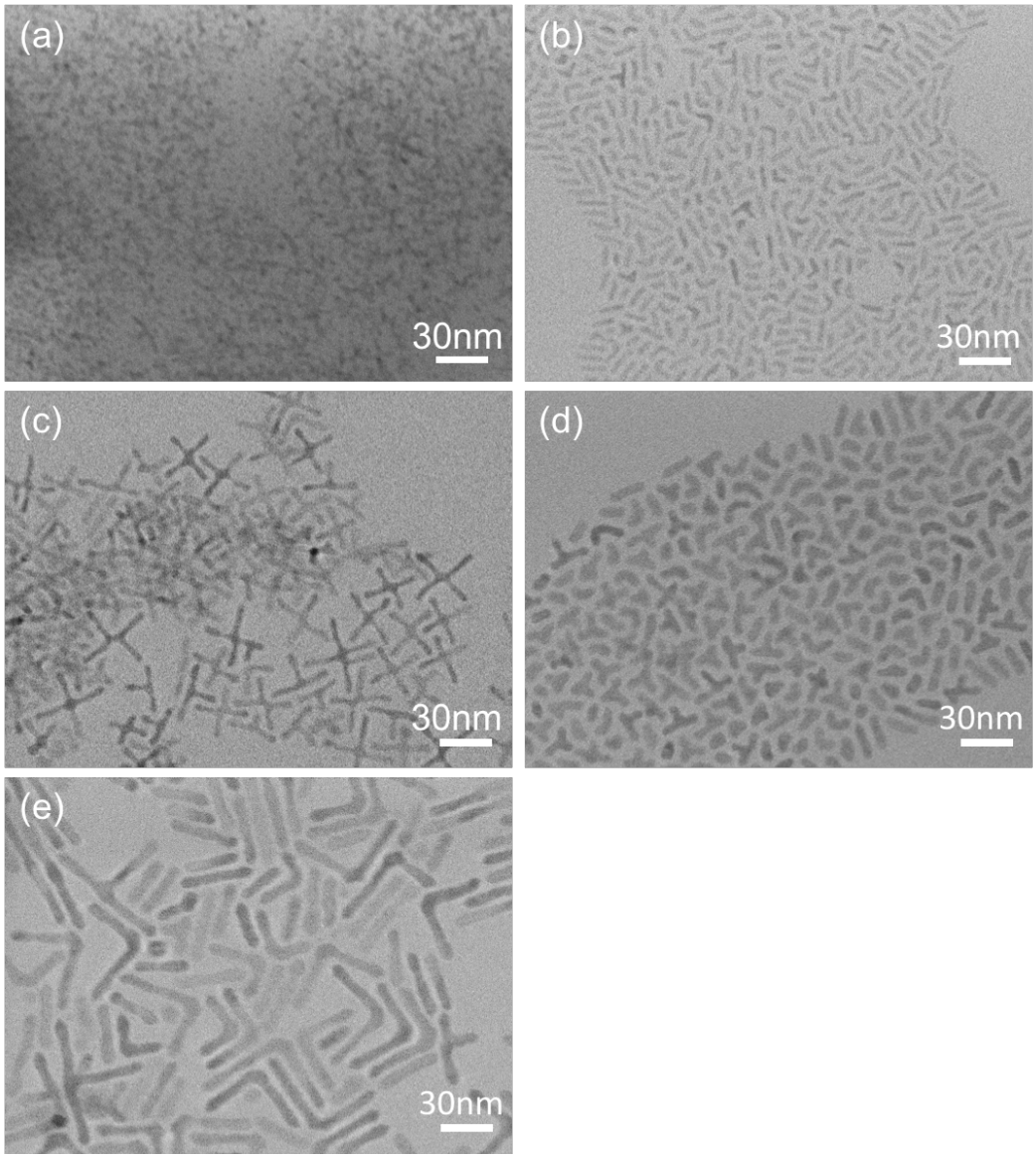

Figure 3.16: TEM images of PbSe nanorods synthesized at different reaction temperatures with fixed time 3 minutes.

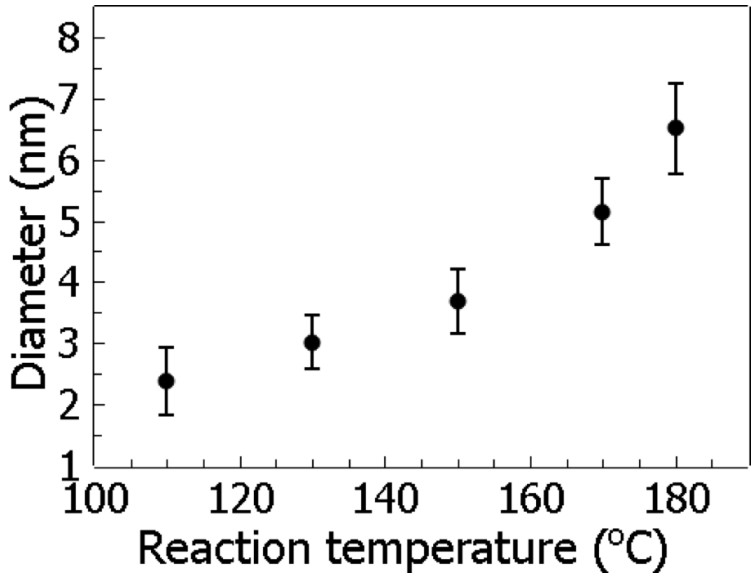

Figure 3.17: Diameter over reaction temperature. The error bar indicates the (±) standard deviation of the diameter.

As the diameter of the nanorods increases, it results in a decrease in the energy gap. It has been observed that as diameter increases the PL of the nanorods has been red-shifted from 1380 nm to 2215 nm as shown in Figure 3.18. The PL peak position for each temperature is summarized in Table 3-1.

Temperature (^{0}C)	PL peak position (nm)
110	1380
130	1625
150	1770
170	2020
180	2215

Table 3-1: PL peak position of each temperature.

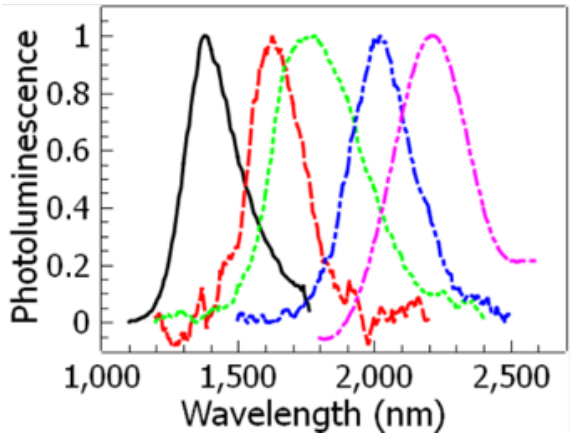

Figure 3.18: PL spectra of PbSe nanorods synthesized at different reaction temperature: 110^{o}C (Black: solid line), 130^{o}C (Red: dashed line), 150^{o}C (Green: dotted line), 170^{o}C (Blue: dot-dashed line) and 180^{o}C (Purple: double-dot-dashed line).

The optical absorption peak of the nanorods was used to calculate energy gap. Energy gap dependence on the diameter nearly follows the diameter$^{-1.5}$ law, which is consistent with calculated results using four band effective-mass model by Bartnik[34] and coworkers.

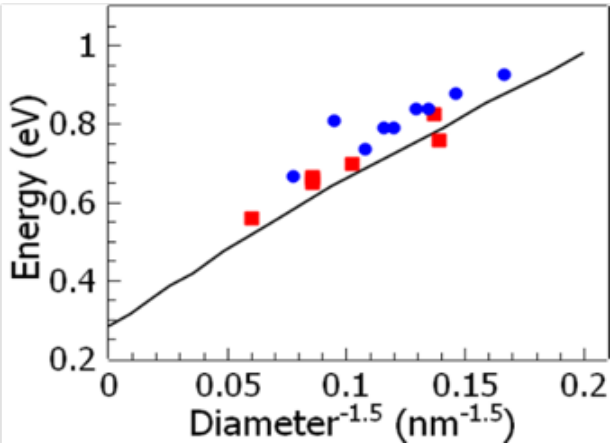

Figure 3.19: Energy gap dependence on the diameter of the nanorods. Red squares: our data, blue dots: Bartnik's data, solid line: Bartnik's calculation.

3.5 EFFECT OF AMOUNT OF CHLOROALKANE ON NANORODS

As we have already discussed that chloroalkane is necessary for the one-dimensional growth. In this chapter, we tried to find the effect of the amount of Chloroalkane. For this, the type of chloroalkane, reaction temperature as well as growth time were fixed. Chloroalkane TCP was used, the final reaction temperature was maintained at 170^0C and growth time was fixed to be 5 minutes.

For 1 ml of TCP, the nanorods were observed along with PL peak. The diameter and the length of nanorods were found to be 5.28 ± 0.26 nm and 32.67 ± 2.86 nm. Usually, in our typical synthesis procedure, we use 1 ml of chloroalkane as a cosolvent.

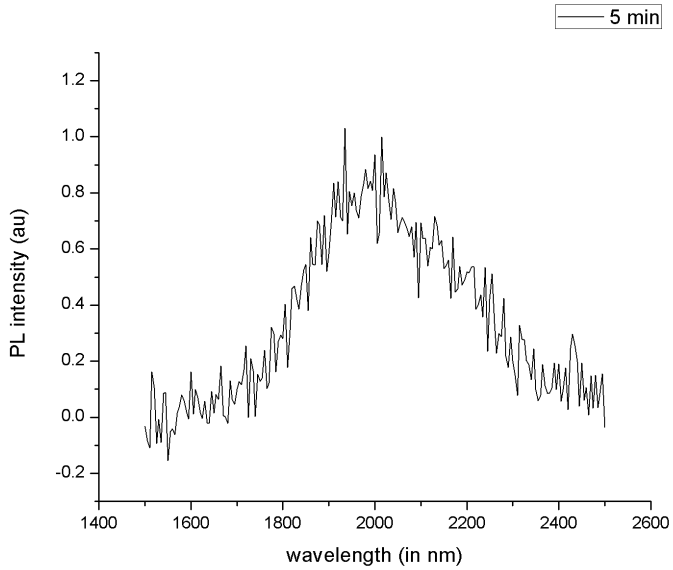

Figure 3.20: PL spectra of PbSe nanorods synthesized using 1 ml of chloroalkane.

As the amount of the Chloroalkane is increased to 2 ml, the size of the nanorods increased by almost the factor of 2. The diameter and length of the NRs were found to be 9.84 ± 1.54 nm and 81.35 ± 4.28 nm. The PL intensity peak for this was not observed. It could be due to the larger size or could be due the range of the detector available in our lab.

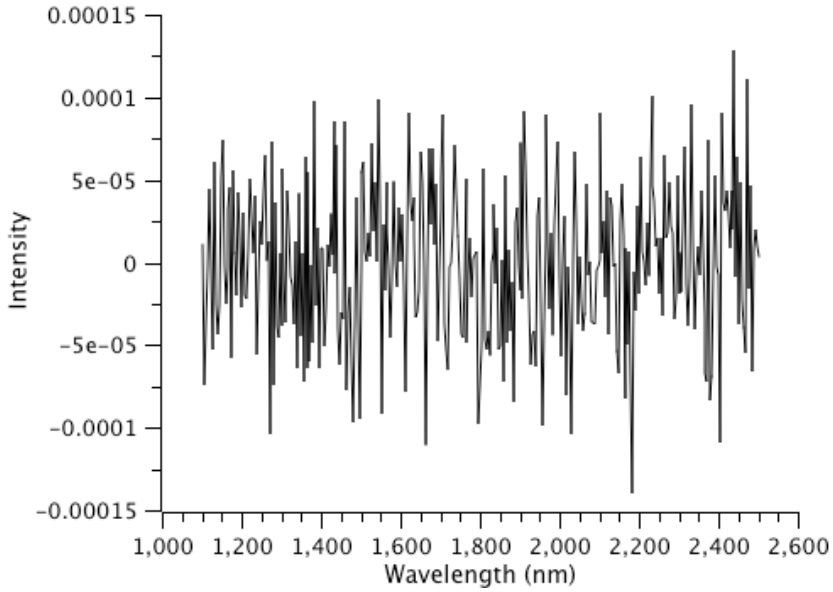

Figure 3.21: PL spectra of PbSe nanorods synthesized using 2 ml of chloroalkane.

Once the amount of Chloroalkane was increased to 3 ml, the irregularly shaped nanocrystals were observed.

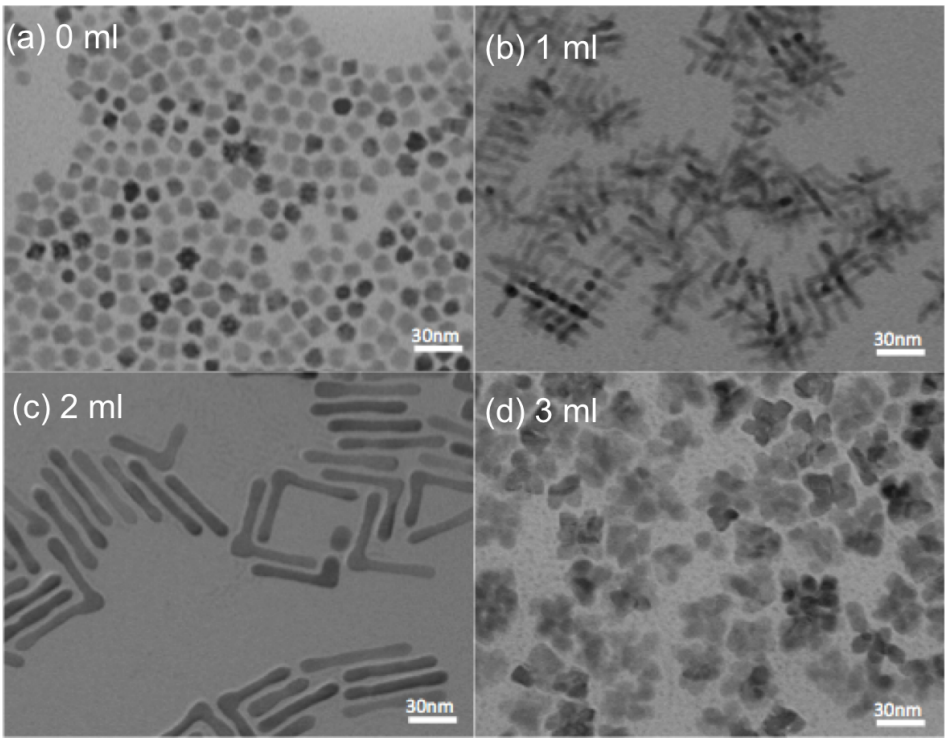

Figure 3.22: TEM images of nanocrystal synthesized using different amount of Chloroalkane.

As the amount of the chloroalkane increases, the reactivity of {110} or {111} facets might have increased due to which the nanorods size has increased by the factor of 2. But after 3 ml of chloroalkane, each facet might have reactivity close enough so that the growth of nanocrystal is in all directions.

3.6 EFFECT OF OLEIC ACID ON THE GROWTH OF NANORODS

In this experimental section, we tried to understand how the changes in Pb:OA ratio affect the growth of the NRs. For this, we fixed the chloroalkane to be TCA, final mixing temperature 130^0C and reaction time 3min.

In typical synthesis procedure the Pb:OA ratio is 1:4. For typical reaction NRs were observed as discussed earlier with PL intensity peak. For this, the length and the diameter of the NRs were found to be 21.26 ± 3.78 nm and 5.27 ± 1.07 nm.

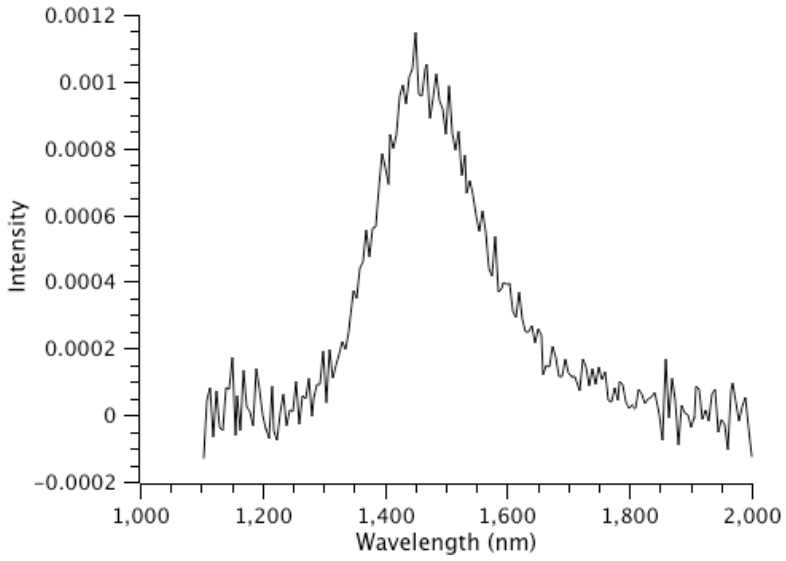

Figure 3.23: PL spectra of PbSe nanorods synthesized using Pb:OA ratio 1:4.

When the Pb:OA ratio is 1:2, cluster-like structure was observed. It could be due to the reason that the oleic acid available for the reaction was not enough for the mixing of lead acetate trihydrate. Due to unmixed Pb-precursor, there might be the presence of acetic acid, which is likely to be responsible for the cluster-like structure.

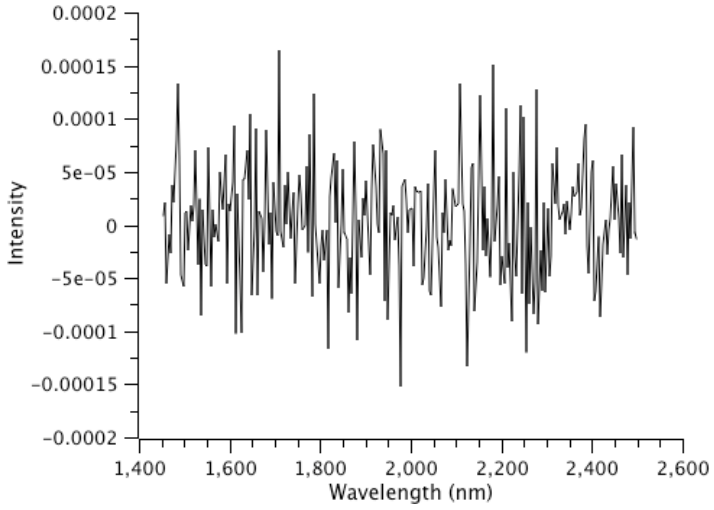

Figure 3.24: PL spectra of PbSe nanorods synthesized using Pb:OA ratio 1:2

When the Pb:OA ratio is 1:8, quantum dots as well as nanorods were observed. The nanorods synthesized have double intensity peak. One peak is around 942 nm and other at 1520 nm. The first peak could be due to the presence of emissive quantum dots. Also, there was not much change in diameter and length of the nanorods. The diameter and length of the NRs were found to be 24.25 ± 4.47 nm and 6.19 ± 1.35 nm.

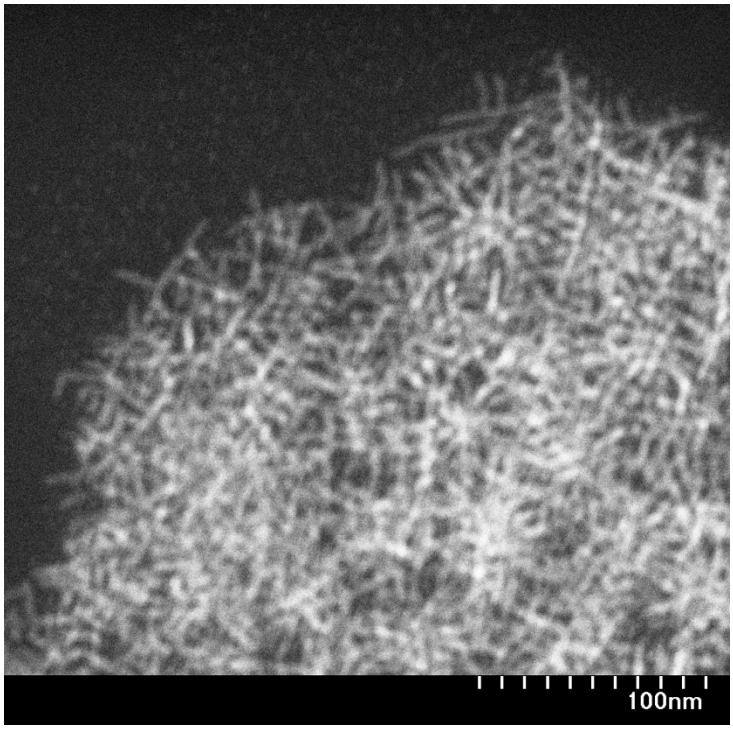

Figure 3.25: TEM image showing the presence of quantum dots and nanorods.

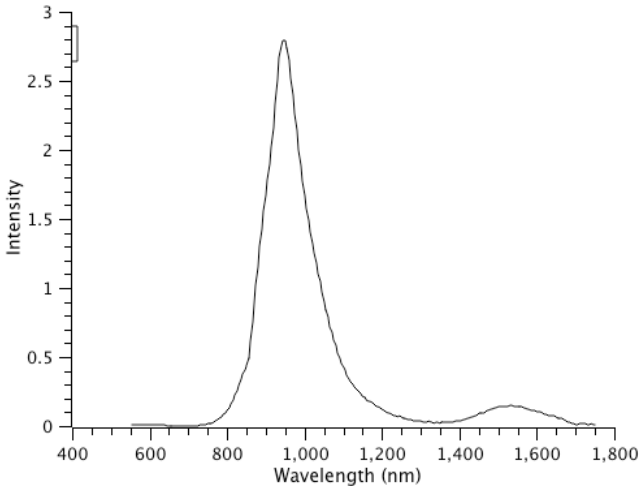

Figure 3.26: PL spectra of PbSe nanorods synthesized using Pb:OA ratio 1:8.

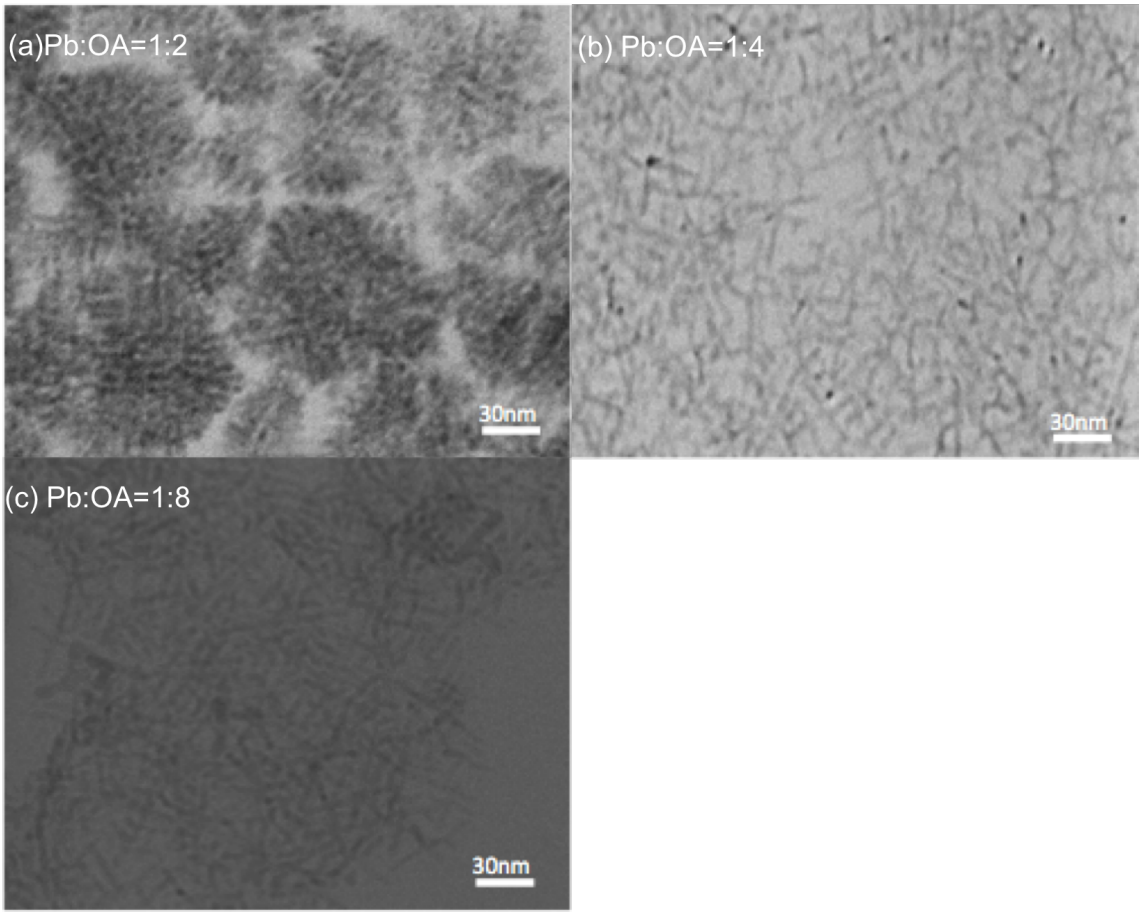

Figure 3.27: TEM images of nanocrystal synthesized using different amount of Pb:OA ratios.

3.7 EFFECT OF ACETIC ACID ON THE GROWTH OF NANORODS

Houtepen et. al[38] found that the presence of the acetic acid in the reaction is responsible for the branching. The synthesis procedure (2.1.1) we developed has lead acetate trihydrate as the Pb-precursor. When it's mixed with oleic acid, we get Pb-oleate as well as acetic acid and water,

$$PbAc_2.3H_2O + 2C_{17}H_{33}COOH \rightarrow Pb(C_{17}H_{33}COO)_2 + 3H_2O + 2HAc$$

Though acetic acid and water are removed from the reaction, it is hard to tell whether all the acetic acid is removed or not. So we modified our synthesis procedure, instead of using lead acetate trihydrate we use lead oxide (PbO). [45]

$$PbO + 2C_{17}H_{33}COOH \rightarrow Pb(C_{17}H_{33}COO)_2 + H_2O$$

The synthesized PbSe nanorods using this method also have narrow emission peak. TEM image confirms the presence of nanorods.

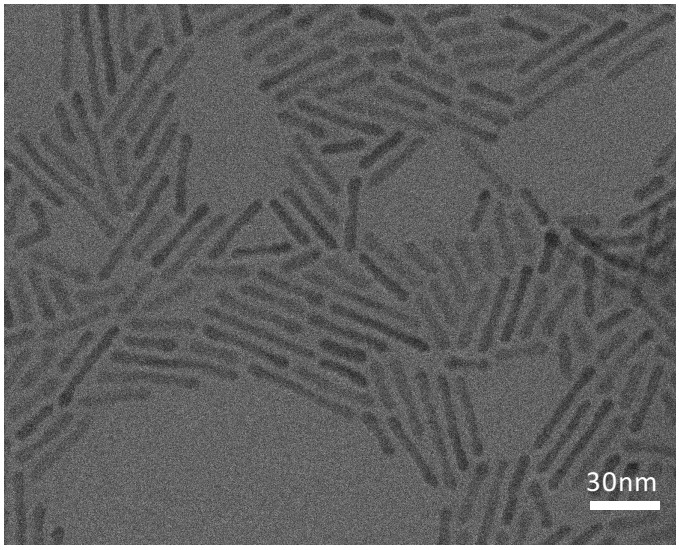

Figure 3.28: TEM image of PbSe nanorods synthesized without acetic acid.

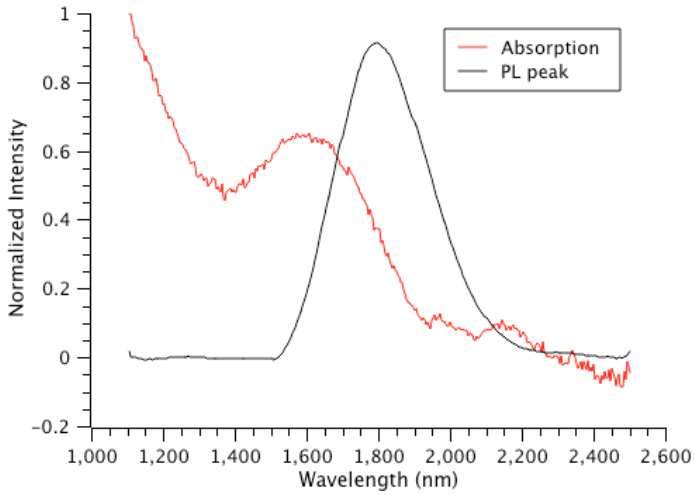

Figure 3.29: Normalized PL and absorption peak.

The procedure discussed on 2.2 was used to understand the effect of acetic acid. As the intentionally added amount of acetic acid increases the color changing time of the reaction became fast as shown in Figure 3.30.

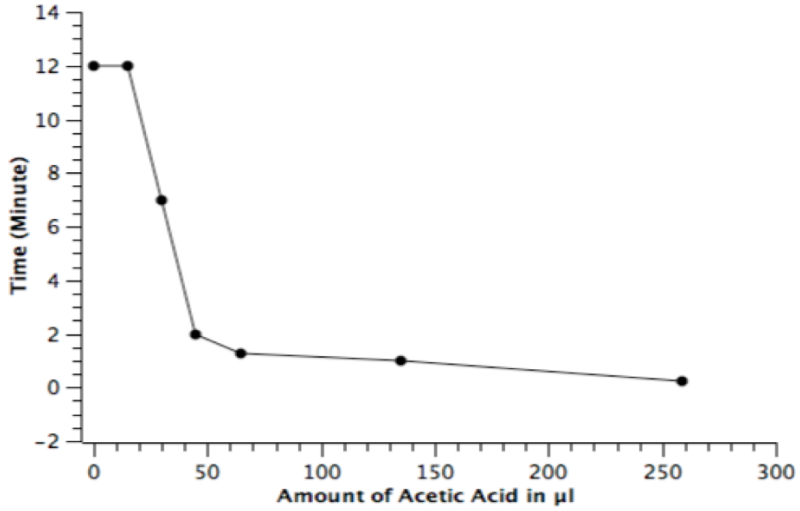

Figure 3.30: Color changing time over amount of acetic acid.

Since the color changing time is directly related to the formation of nanocrystals and how fast the nanocrystals grows. That means if color-changing time is slow, then nanocrystal growth is also

slow and vice versa. As shown in Figure 3.30, there is a notable difference in color changing time. So, we defined a term “growth index”. For typical synthesis, without acetic acid, the color changing time is about 12 minute and we take our first sample around 1.5 hours. So we divided sample-taking time by the color changing time, which we named as growth index. So, growth index is 7.5. We fixed growth index range 7-8. Throughout the experiments, we fixed reaction time based on that growth index range.

Amount of acetic acid (In μl)	Color changing time (In minute)	Reaction time (In minute)
0	12	90
15	12	90
30	7	60
45	2	16
65	1.25	10
125	1	5
259	0.25	2

Table 3-2: Summarization of reaction time based on color changing time as amount of acetic acid increases.

We found that the presence of acetic acid has a greater impact on the formation of PbSe nanorods. After 30 μl of acetic acid the nanorods shape changes to the more cluster-like structure. The Threshold for the formation of PbSe NRs is found to be 30 μl of acetic acid. The TEM images below shows the effect of acetic acid on PbSe NRs.

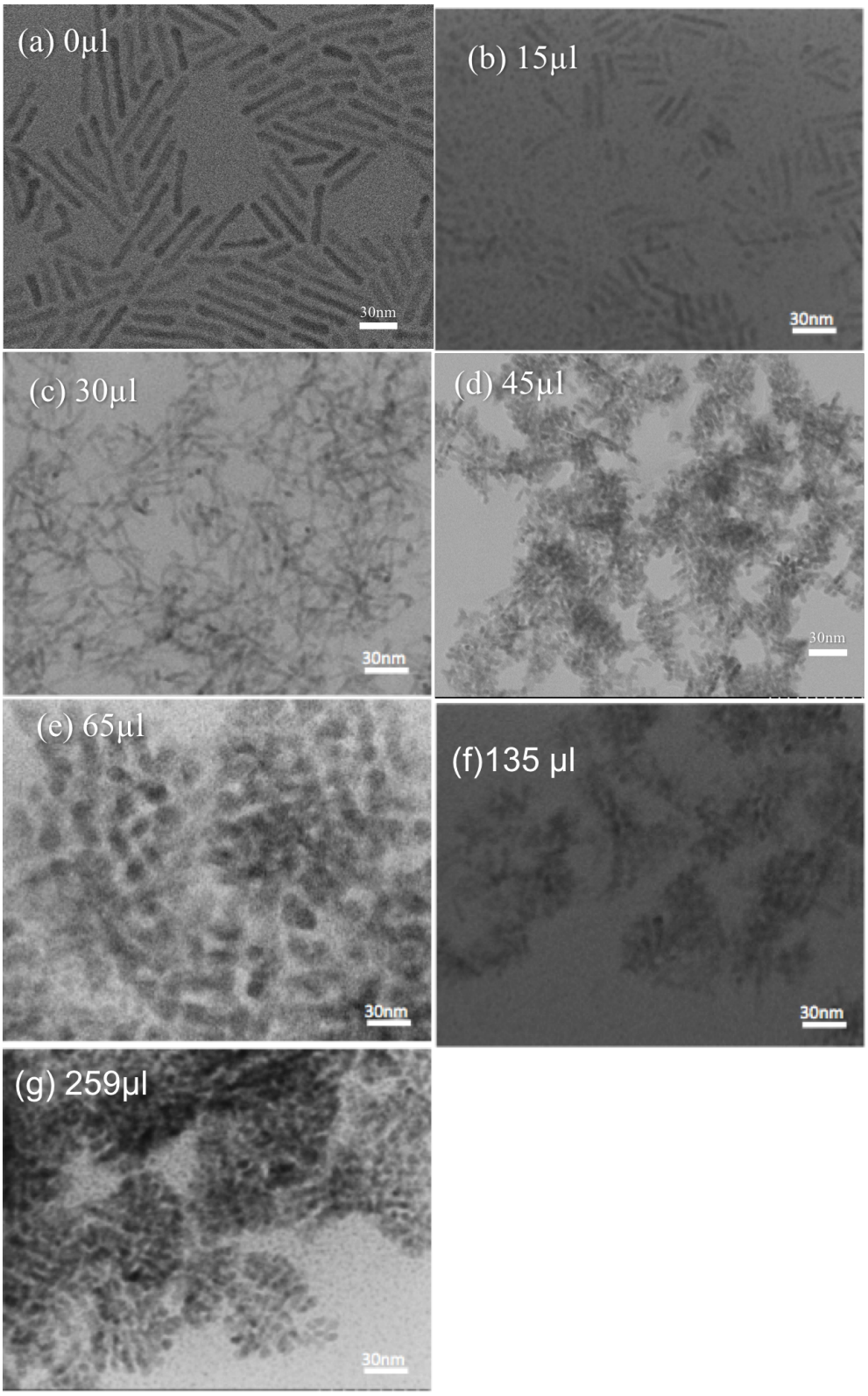

Figure 3.31: TEM images of NCs synthesized using different amount of acetic acid

3.8 EFFECT OF WATER ON THE GROWTH OF NANORODS

Boercker et al.[37] have found that as the amount of water increases the branching increases and also aspect ratio of the nanorods decreases. We use the method as described in section 2.2. Our result was different from the results from Boercker. For 40 µl and 120 µl of water mixture of quantum dots and nanorods were observed but for 80 µl and 240 µl of water, we didn't observe any presence of quantum dots. The aspect ratio of the NRs has been decreased. Without the presence of water aspect ratio was around 8.08, but when we use water it has been decreased to about 4. The aspect ratio of nanorods is almost same once water is added. There is redshift in PL up to 120 µl of water indicating the increase in diameter of nanorods or quantum dots.

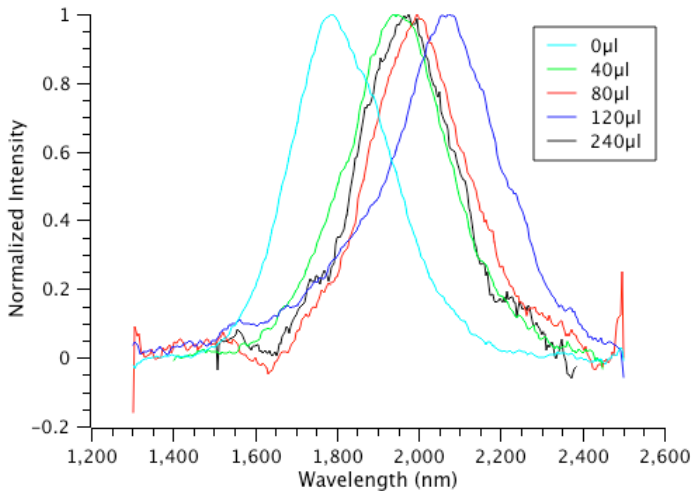

Figure 3.32: PL spectra of PbSe NCs synthesized using different amount of water.

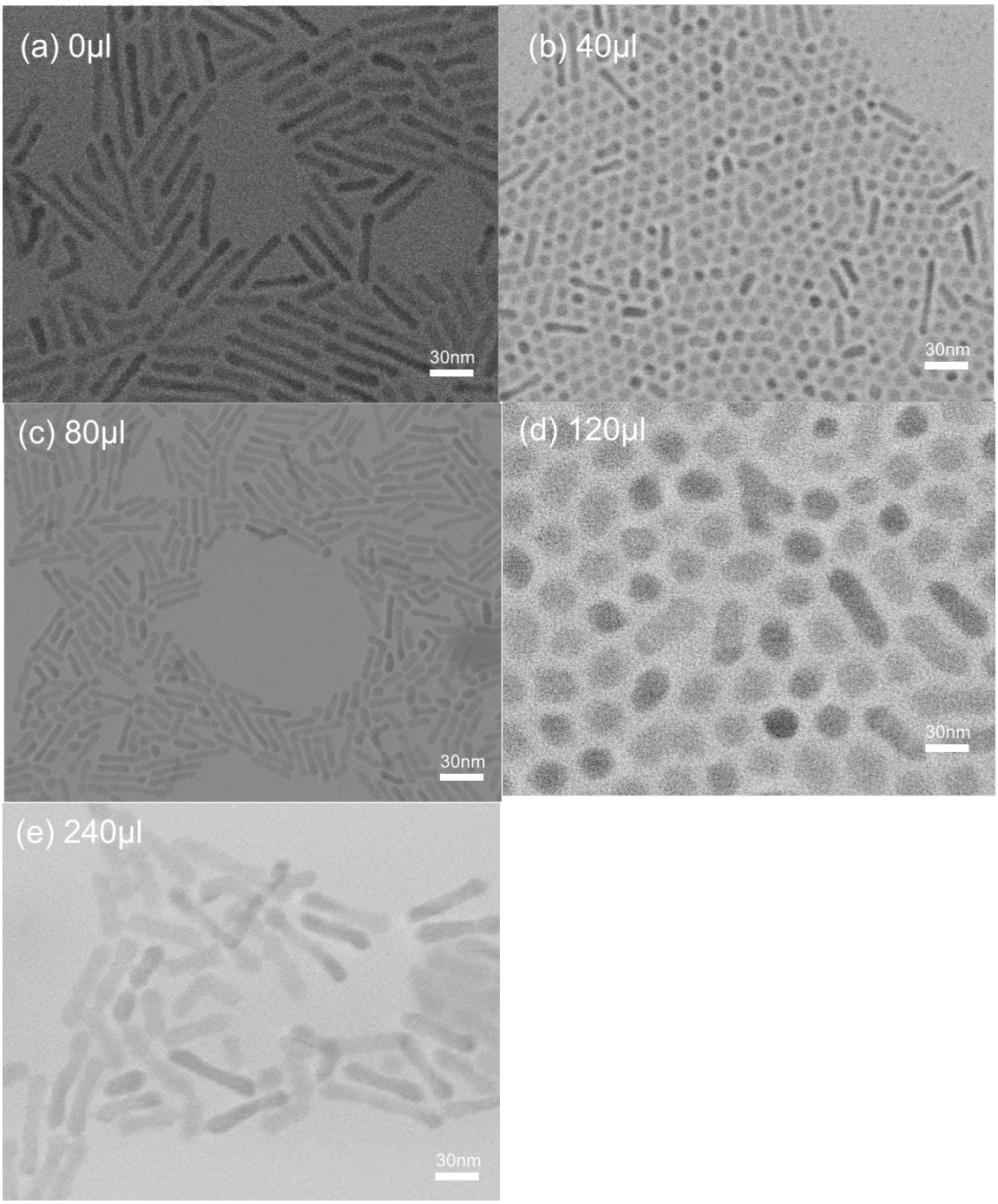

Figure 3.33: TEM images of NCs synthesized using different amount of water.

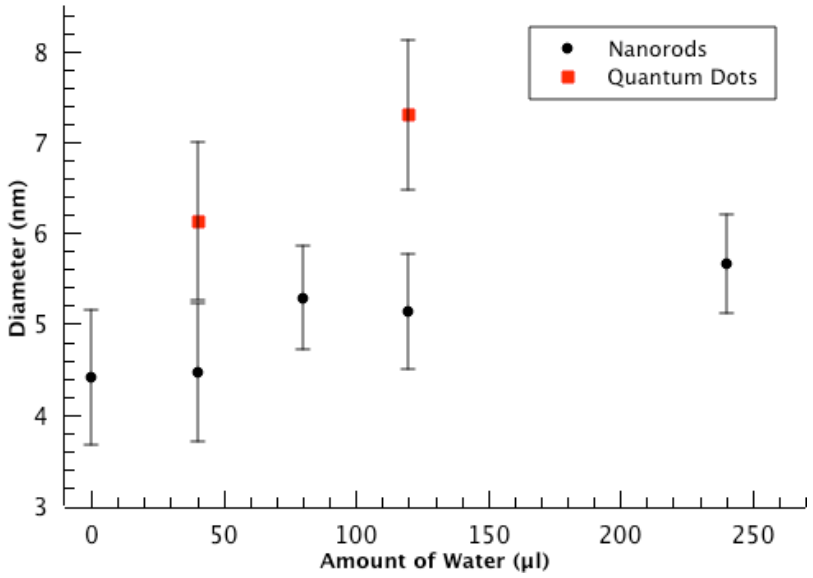

Figure 3.34: Diameter over amount of water. Here black dots are for NR only and red square is for quantum dots.

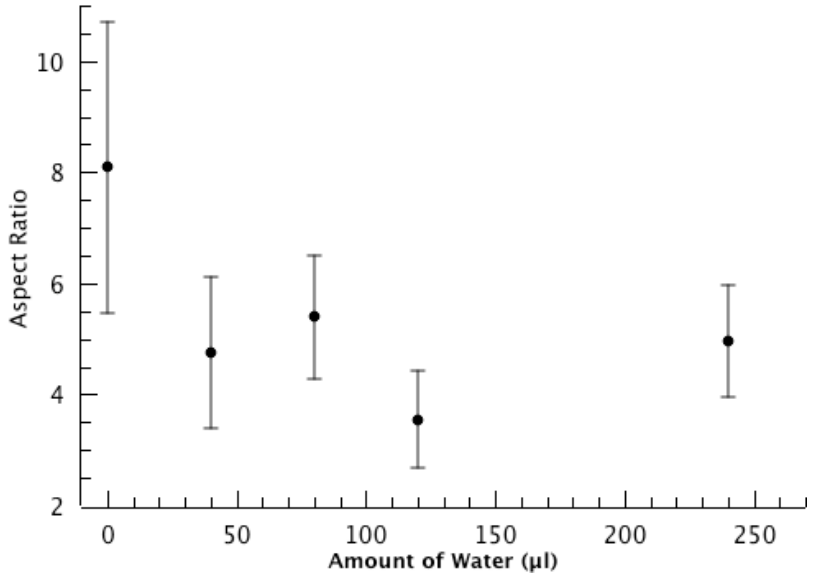

Figure 3.35: Aspect ratio over amount of water.

3.9 CONCLUSION

In summary, we have developed the synthesis method and studied the growth mechanism of PbSe nanorods. We found that Chloroalkane is required for the one-dimensional growth. Temperature and time have a greater role for the tuning of the diameter of the nanorods. By tuning the diameter, we can get novel optical properties. Also, the amount of chloroalkane has an important role in the formation of PbSe nanorods. Usually, 1 ml of chloroalkane is better as they give emissive nanorods compared to 2 ml. More than 2 ml of chloroalkane gives irregularly shaped structure. The ratio of Pb:OA affects the formation of nanorods. The presence of acetic acid in precursor solution has the great impact on the formation of PbSe nanorods. If more than 30 μl of acetic acid is present in the Pb- precursor then clusters like structures will be formed. Also, as the amount of the water increases, nanorods aspect ratio decreases.

CHAPTER 4: FUTURE DIRECTIONS

4.1 BRANCHLESS NANORODS

In this project, we have developed one new synthesis method as described in 2.1.2. Since success rate of this method is higher compared to 2.1.1, in future we will be taking this synthesis method and try to tune diameter and length of the nanorods. The absence of acetic acid makes it easier to change parameters like Pb to Se ratio, OA to Pb ratio etc. In current typical methods Pb:Se ratio is 14:1, we are trying to reduce that ratio so that it will be cost-effective for industrial applications

4.2 PbSe/CdSe NANORODS HETEROSTRUCTURES

To improve the surface passivation[59, 60] of the PbSe nanorods, we are currently working on adding CdSe-shell around the core of PbSe nanorods. This core/shell structure is achieved through the cation exchange. In this method, the morphology of the nanorods remains same and the total diameter of core/shell remains same as of original nanorods. Our recent result shows that the morphology of the nanorods has remained same and we have observed the blue-shift in PL peak indicating the formation of shell or shrinking of the core.

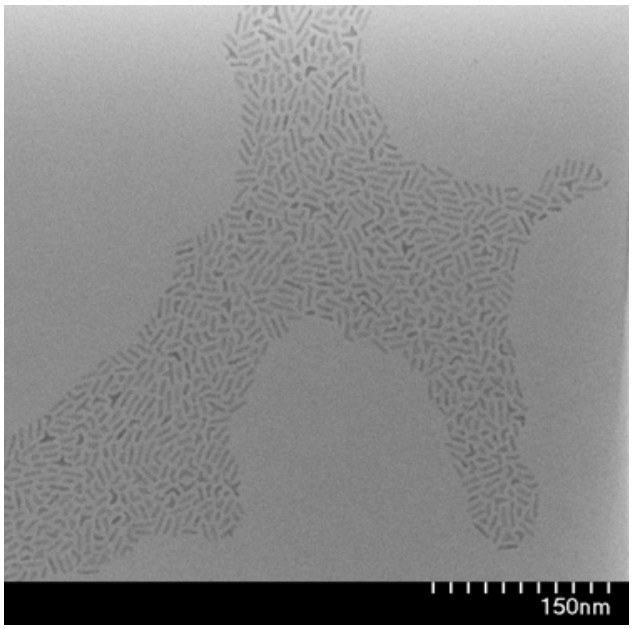

Figure 4.1: TEM image of PbSe nanorods.

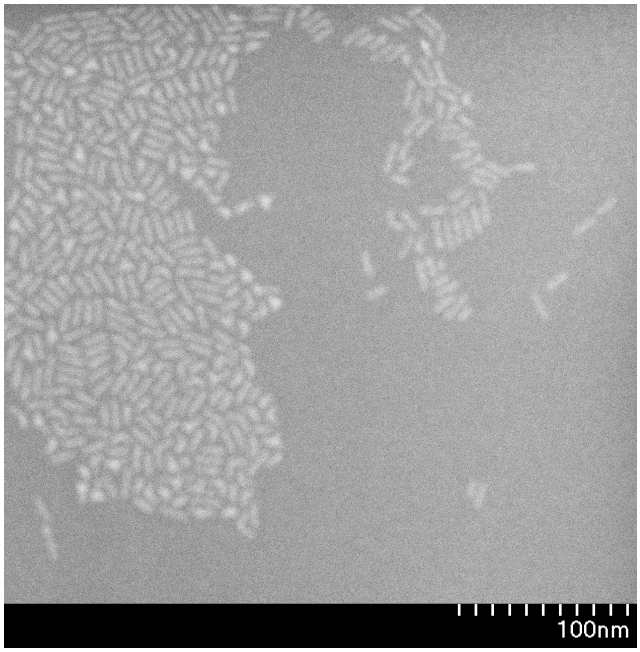

Figure 4.2: TEM image after core/shell synthesis.

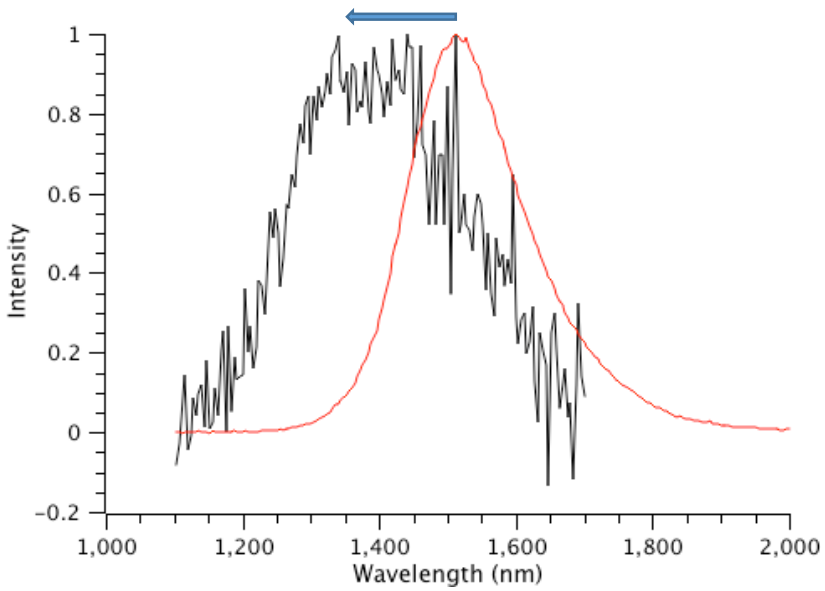

Figure 4.3: Normalized PL spectra of original nanorods (red) and core/shell structure (black). Blue line is indicating the blue-shift in PL

REFERENCES

1. Binnig G, Rohrer H. Scanning tunneling microscopy. Surf Sci 1983;126(1):236-44.

2. Bocking S. The smallest revolution: We need to learn more about nanomaterials before they get too far under our skin. Alternatives Journal 2008;34(4):30-3.

3. Lin X. From nanocrystals to nanocrystal superlattices: Synthesis and properties. ; 1999.

4. Misra SK, Tetley TD, Thorley A, Boccaccini AR, Valsami-Jones E. Engineered nanomaterials. In: Pollutants, human health and the environment: A risk based approach. John Wiley & Sons, Ltd; 2012.

5. Ahmad R, Tripathy N, Hahn Y. Highly stable urea sensor based on ZnO nanorods directly grown on ag/glass electrodes. Sensors Actuators B: Chem 2014;194:290-5.

6. Marinakos SM, Chen S, Chilkoti A. Plasmonic detection of a model analyte in serum by a gold nanorod sensor. Anal Chem 2007;79(14):5278-83.

7. Xu X, Ying Y, Li Y. Gold nanorods based LSPR biosensor for label-free detection of alpha-fetoprotein. Procedia Engineering 2011;25:67-70.

8. Wang C, Irudayaraj J. Gold nanorod probes for the detection of multiple pathogens. Small 2008;4(12):2204-8.

9. Ito Y, Fukusaki E. DNA as a 'Nanomaterial'. J Molec Catal B 2004 6/1;28(4–6):155-66.

10. Zhao Z. Functional DNA nanomaterials. Arizona-USA: Arizona State University,; 2013.

11. Schaefer HE. Nanoscience. Berlin ; London : Springer; 2010.

12. Kittel C. Introduction to solid state physics. seventh ed. New York: John Wiley & Sons, Inc.; 1996.

13. Myasnikov E, Myasnikova A. Band theory of semiconductors and autolocalization of electrons. Physics Letters A 2001;286(2):210-6.

14. Schmid G. Nanoparticles: From theory to application. John Wiley & Sons; 2011. .

15. Machol J, Wise F, Patel R, Tanner D. Optical studies of IV–VI quantum dots. Physica A: Statistical Mechanics and its Applications 1994;207(1):427-34.

16. Alivisatos AP. Semiconductor clusters, nanocrystals, and quantum dots. Science 1996;271(5251):933.

17. Jiao J, Liu X, Gao W, Wang C, Feng H, Zhao X, Chen L. Synthesis of PbS nanoflowers by biomolecule-assisted method in the presence of supercritical carbon dioxide. Solid State Sciences 2009;11(5):976-81.

18. Padilha LA, Stewart JT, Sandberg RL, Bae WK, Koh W, Pietryga JM, Klimov VI. Aspect ratio dependence of auger recombination and carrier multiplication in PbSe nanorods. Nano Letters 2013;13(3):1092-9.

19. Yang J, Hyun B, Basile AJ, Wise FW. Exciton relaxation in PbSe nanorods. ACS Nano 2012;6(9):8120-7.

20. Placencia D, Boercker JE, Foos EE, Tischler JG. Synthesis and optical properties of PbSe nanorods with controlled diameter and length. The Journal of Physical Chemistry Letters 2015;6(17):3360-4.

21. Kramer IJ, Sargent EH. The architecture of colloidal quantum dot solar cells: Materials to devices. Chem Rev 2013;114(1):863-82.

22. Oh SJ, Berry NE, Choi J, Gaulding EA, Lin H, Paik T, Diroll BT, Muramoto S, Murray CB, Kagan CR. Designing high-performance PbS and PbSe nanocrystal electronic devices through stepwise, post-synthesis, colloidal atomic layer deposition. Nano Letters 2014;14(3):1559-66.

23. Yang J, Hyun B, Basile AJ, Wise FW. Exciton relaxation in PbSe nanorods. ACS Nano 2012;6(9):8120-7.

24. Yoon W, Boercker JE, Lumb MP, Placencia D, Foos EE, Tischler JG. Enhanced open-circuit voltage of PbS nanocrystal quantum dot solar cells. Scientific Reports 2013;3.

25. Zhang J, Gao J, Church CP, Miller EM, Luther JM, Klimov VI, Beard MC. PbSe quantum dot solar cells with more than 6% efficiency fabricated in ambient atmosphere. Nano Letters 2014;14(10):6010-5.

26. Aerts M, Spoor FC, Grozema FC, Houtepen AJ, Schins JM, Siebbeles LD. Cooling and auger recombination of charges in PbSe nanorods: Crossover from cubic to bimolecular decay. Nano Letters 2013;13(9):4380-6.

27. Htoon H, Hollingsworth J, Dickerson R, Klimov V. Effect of zero-to one-dimensional transformation on multiparticle auger recombination in semiconductor quantum rods. Phys Rev Lett 2003;91(22):227401.

28. Cunningham PD, Boercker JE, Placencia D, Tischler JG. Anisotropic absorption in PbSe nanorods. ACS Nano 2013;8(1):581-90.

29. Placencia D, Boercker JE, Foos EE, Tischler JG. Synthesis and optical properties of PbSe nanorods with controlled diameter and length. The Journal of Physical Chemistry Letters 2015;6(17):3360-4.

30. Cunningham PD, Boercker JE, Foos EE, Lumb MP, Smith AR, Tischler JG, Melinger JS. Enhanced multiple exciton generation in quasi-one-dimensional semiconductors. Nano Letters 2011;11(8):3476-81.

31. Fu H, Tsang S. Infrared colloidal lead chalcogenide nanocrystals: Synthesis, properties, and photovoltaic applications. Nanoscale 2012;4(7):2187-201.

32. Murphy JE, Beard MC, Norman AG, Ahrenkiel SP, Johnson JC, Yu P, Micic OI, Ellingson RJ, Nozik AJ. PbTe colloidal nanocrystals: Synthesis, characterization, and multiple exciton generation. J Am Chem Soc 2006;128(10):3241-7.

33. Tischler J, Kennedy T, Glaser E, Efros AL, Foos E, Boercker J, Zega T, Stroud R, Erwin S. Band-edge excitons in PbSe nanocrystals and nanorods. Physical Review B 2010;82(24):245303.

34. Bartnik A, Efros AL, Koh W, Murray C, Wise F. Electronic states and optical properties of PbSe nanorods and nanowires. Physical Review B 2010;82(19):195313.

35. Koh W, Bartnik AC, Wise FW, Murray CB. Synthesis of monodisperse PbSe nanorods: A case for oriented attachment. J Am Chem Soc 2010;132(11):3909-13.

36. Cho K, Talapin DV, Gaschler W, Murray CB. Designing PbSe nanowires and nanorings through oriented attachment of nanoparticles. J Am Chem Soc 2005;127(19):7140-7.

37. Boercker JE, Foos EE, Placencia D, Tischler JG. Control of PbSe nanorod aspect ratio by limiting phosphine hydrolysis. J Am Chem Soc 2013;135(40):15071-6.

38. Houtepen AJ, Koole R, Vanmaekelbergh D, Meeldijk J, Hickey SG. The hidden role of acetate in the PbSe nanocrystal synthesis. J Am Chem Soc 2006;128(21):6792-3.

39. Dai Q, Zhang Y, Wang Y, Wang Y, Zou B, Yu WW, Hu MZ. Ligand effects on synthesis and post-synthetic stability of PbSe nanocrystals. The Journal of Physical Chemistry C 2010;114(39):16160-7.

40. Singh SC, Zeng H, Yang S, Cai W, Hong M, Chen G, Chong TC. Nanomaterials: Laser-Based processing in liquid media. Nanomaterials: Processing and Characterization with Lasers 2012:317-494.

41. Mignot A, Truillet C, Lux F, Sancey L, Louis C, Denat F, Boschetti F, Bocher L, Gloter A, Stéphan O. A Top-Down synthesis route to ultrasmall multifunctional Gd-Based silica nanoparticles for theranostic applications. Chemistry–A European Journal 2013;19(19):6122-36.

42. Wei Q. Synthesis, properties and applications of nanorods and nanowires. ; 2001.

43. Oliver CR, Westrick W, Koehler J, Brieland-Shoultz A, Anagnostopoulos-Politis I, Cruz-Gonzalez T, Hart AJ. Robofurnace: A semi-automated laboratory chemical vapor deposition system for high-throughput nanomaterial synthesis and process discovery. Rev Sci Instrum 2013;84(11):115105.

44. Bhandari GB, Subedi K, He Y, Jiang Z, Leopold M, Reilly N, Lu HP, Zayak AT, Sun L. Thickness-controlled synthesis of colloidal PbS nanosheets and their thickness-dependent energy gaps. Chemistry of Materials 2014;26(19):5433-6.

45. Zhang H, Savitzky BH, Yang J, Newman JT, Perez KA, Hyun B, Kourkoutis LF, Hanrath T, Wise FW. Colloidal synthesis of PbS and PbS/CdS nanosheets using acetate-free precursors. Chemistry of Materials 2015;28(1):127-34.

46. **Photoluminescence explained** [Internet]; c2016 [cited 2016 05/.24]. Available from: http://www.renishaw.com/en/photoluminescence-explained--25809.

47. Bhandari GB. Synthesis and ab-initio simulations of colloidal PbS nanosheets. Bowling Green State University; 2014.

48. Kandel SR. Control of shape change of PbSe nano structure by chloroalkane. Bowling Green State University; 2015.

49. Khan S. Colloidai PbS and PbS/CdS nanosheets heterostructure. Bowling Green State University; 2015.

50. Subedi K. Synthesis and characterization of PbS nanosheets. Bowling Green State University; 2014.

51. Wenzel TJ. Douglas A. skoog, donald M. west, F. james holler, and stanley R. crouch: Fundamentals of analytical chemistry. Analytical and Bioanalytical Chemistry 2013;405(25):7903.

52. Berezin MY, Achilefu S. Fluorescence lifetime measurements and biological imaging. Chem Rev 2010;110(5):2641-84.

53. Gerdes F, Volkmann M, Schliehe C, Bielewicz T, Klinke C. Sculpting of lead sulfide nanoparticles by means of acetic acid and dichloroethane. Zeitschrift Für Physikalische Chemie 2015;229(1-2):139-51.

54. Schliehe C, Juarez BH, Pelletier M, Jander S, Greshnykh D, Nagel M, Meyer A, Foerster S, Kornowski A, Klinke C, et al. Ultrathin PbS sheets by two-dimensional oriented attachment. Science 2010 Jul 30;329(5991):550-3.

55. Skrabalak SE, Xia Y. Pushing nanocrystal synthesis toward nanomanufacturing. ACS Nano 2009;3(1):10-5.

56. Bealing CR, Baumgardner WJ, Choi JJ, Hanrath T, Hennig RG. Predicting nanocrystal shape through consideration of surface-ligand interactions. ACS Nano 2012;6(3):2118-27.

57. Lee S, Jun Y, Cho S, Cheon J. Single-crystalline star-shaped nanocrystals and their evolution: Programming the geometry of nano-building blocks. J Am Chem Soc 2002;124(38):11244-5.

58. Choi H, Ko J, Kim Y, Jeong S. Steric-hindrance-driven shape transition in PbS quantum dots: Understanding size-dependent stability. J Am Chem Soc 2013;135(14):5278-81.

59. Manna L, Scher EC, Li L, Alivisatos AP. Epitaxial growth and photochemical annealing of graded CdS/ZnS shells on colloidal CdSe nanorods. J Am Chem Soc 2002;124(24):7136-45.

60. Pietryga JM, Werder DJ, Williams DJ, Casson JL, Schaller RD, Klimov VI, Hollingsworth JA. Utilizing the lability of lead selenide to produce heterostructured nanocrystals with bright, stable infrared emission. J Am Chem Soc 2008;130(14):4879-85.

APPENDIX A: EXPERIMENTAL DETAILS OF PbSe/CdSe HETEROSTRUCTURE

Cd-precursor was prepared by taking 0.2525 gm of CdO, 1.5 ml of oleic acid and 4 ml of diphenyl ether in one three-necked flask. The mixture was heated to 255^0C under nitrogen flow and once the solution becomes clear, then it's temperature was dropped to 155^0C. At the same time, on another flask 3ml of nanorods sample, which was dispersed on Toluene, was taken and 6 ml of extra toluene was added and the nanorods mixture was heated to 100^0C. Once the nanorods mixture reaches to 100^0C, Cd-precursor was mixed. The sample was taken after 5 minutes and quenched in toluene to stop further growth. Sample collected were cleaned using toluene and methanol by centrifuging at 3.5 Krpm for 5 minutes.[49]